T.C.

ALTINBAS UNIVERSITY

Institute of Graduate Studies

Electrical and Computer Engineering

DESIGN OF A MPPT SYSTEM BASED ON MODIFIED GREY WOLF OPTIMIZATION ALGORITHM IN PHOTOVOLTAIC SYSTEM UNDER PARTIALLY SHADED CONDITION

Hatem Khalifa Emhmed Ghazal

Master of Science

Supervisor

Asst.Prof. Muhammad Ilyas

Istanbul, 2021

DESIGN OF A MPPT SYSTEM BASED ON MODIFIED GREY WOLF OPTIMIZATION ALGORITHM IN PHOTOVOLTAIC SYSTEM UNDER PARTIALLY SHADED CONDITION

by

Hatem Khalifa Emhmed Ghazal

Electrical and Computer Engineering

Submitted to the Institute of Graduate Studies

in partial fulfillment of the requirements for the degree of

Master of Science

ALTINBAŞ UNIVERSITY

2021

The thesis titled "DESIGN OF A MPPT SYSTEM BASED ON MODIFIED GREY WOLF OPTIMIZATION ALGORITHM IN PHOTOVOLTAIC SYSTEM UNDER PARTIALLY SHADED CONDITION" prepared and presented by "Hatem Khalifa Emhmed Ghazal" was accepted as a Master of Science Thesis in Department.

____

Asst.Prof. Muhammad Ilyas

Supervisor

Thesis Defense Jury Members:

Asst. Prof. Muhammad Ilyas	School of Engineering and Natural Sciences, Altinbas University	____________________
Asst. Prof. Abdullah Abdu Ibrahim	School of Engineering and Natural Sciences, Altinbas University	____________________
Asst. Prof. Akhtar Jamil	Computer Engineering, Sabahattin Zaim University	____________________

I certify that this thesis satisfies all the requirements as a thesis for the degree of Master of Science.

Approval Date of Institute of Graduate Studies:

____/____/____

I hereby declare that all information in this document has been obtained and presented in accordance with academic rules and ethical conduct. I also declare that, as required by these rules and conduct, I have fully cited and referenced all material and results that are not original to this work.

Hatem Khalifa Emhmed Ghazal

Signature

ACKNOWLEDGEMENTS

I might want to thank my administrator Asst.Prof. Muhammar Ilyas Please let me express my profound feeling of appreciation and gratefulness to you for the information direction and unrestricted help you have given me. I want you to enjoy all that life has to offer and further achievement and accomplishments throughout your life.

ABSTRACT

DESIGN OF A MPPT SYSTEM BASED ON MODIFIED GREY WOLF OPTIMIZATION ALGORITHM IN PHOTOVOLTAIC SYSTEM UNDER PARTIALLY SHADED CONDITION

Hatem Khalifa Emhmed Ghazal

M.Sc., Electrical and Computer Engineering, Altınbaş University

Supervisor: Asst.Prof. Muhammad Ilyas

Date: March 2021

Pages: 87

The device is not generating pollution and can be built anywhere even in remote areas, and photovoltaics are becoming very common. Nevertheless, it is difficult to achieve optimal and reliable power by using photovoltaics. So, facing these difficulties, this article proposes to monitor the photovoltaic system's global optimum power point for partial shading with a Modified Gray Wolf Optimizer (MGWO) based maximum power point tracking algorithm. A PV device mathematical model is developed using a single model and MGWO is used to measure the world's maximum power point. A photovoltaic system includes deciding which converter is used to increase photovoltaic power generation. The MPPT architecture uses modified gray wolf optimization algorithm to quickly track the output power and reduce photovoltaic oscillations. The efficiency of the maximum power tracker is better than the GWO algorithm of up to 0,4 s with the modified gray wolf optimization algorithm. Converters are used to resolve the power losses often occurring in PV systems with a soft-buck converter process. The output of the power generator is greater than the soft-switching buck converter. If the performance of PV systems is compared with the gray wolf optimization algorithm Increased, the incidence of the conductance algorithm increases.

Keywords: Grey Wolf Optimization (GWO), Maximum Power Point Tracking (MPPT), Partial Shading Conditions (PSC), Photovoltaic (PV)

TABLE OF CONTENTS

Pages

LIST OF TABLES

Pages

LIST OF FIGURES

Pages

LIST OF ABBREVIATIONS

GWO	:	Grey Wolf Optimization
MPP	:	Maximum Power Point
MPPT	:	Maximum Power Point Tracking
P&O	:	Perturb and Observe
PSC	:	Partial Shading Condition
PSO	:	Particle Swarm Optimization
PSOGSA	:	Particle Swarm Optimization Gravitational Search Algorithm
RDPSO	:	Random Drift Particle Swarm Optimization

1. INTRODUCTION

1.1 PHOTOVOLTAIC POWER GENERATION

The increased fossil-fuel and environmental demands, renewable energy, for instance solar energy, wind, hydropower, geothermal energy, etc. has been used in massive ways [1]. Photovoltaic (PV) energy generation has become more and more indispensable as an unconventional source for electricity generation [1]:

•No emissions and waste • low maintenance costs • lack of rotatable pieces • Electricity storage without long lines of transmission.

The term photovoltaic means light and voltaic, which is a combination of two terms which means electricity generation. PV technology deals with the development of solar irradiance electricity. A photovoltaic solar photovoltaic cell is a system that directly transforms the energy in sunlight into electricity [2][3]. Figure 1.1 displays the world photovoltaic growth scenario statistics.

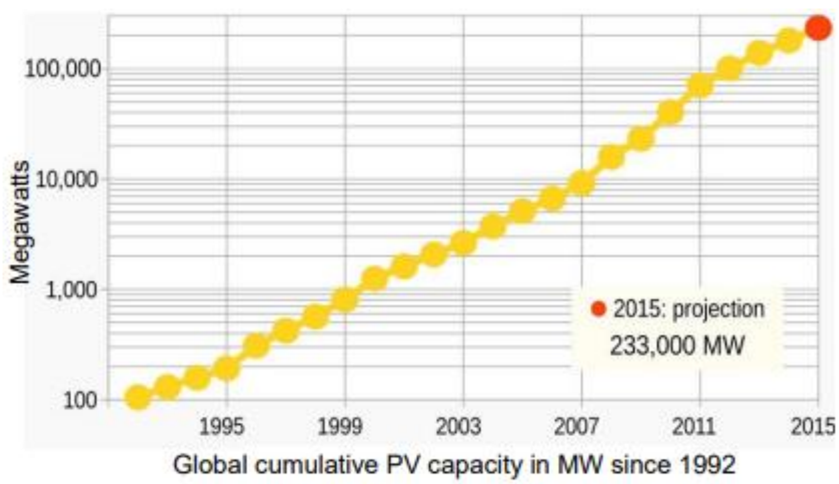

Figure 1.1: Global scenario of PV development [1]

1.2 SOLAR AS A CLEAN RENEWABLE ENERGY

Removable sources of energy are being used due to the growing demand for energy in the industry and the domestic sector. There are also exhaustive and polluting drawbacks of non-renewable sources of energy. Photovoltaic energy has many (similar) advantages (e.g., pollution-free, simple to manage, no carbon emissions and no fuel costs) among different renewable sources. Due. The shadow of trees, buildings and towers, clouds and dust also add partly to the shade. The PV array exhibits local and global power picks under Partial Shading Condition (PSC). The key challenge in partly shading conditions is to map the global power peak. These problems will be resolved, and the overall Output Peak managed by determining the best service value for the boost converter in order to extract the maximum PV array output.

1.3 NECESSITY OF MAXIMUM POWER POINT TRACKING (MPPT)

There is a rising global need for sustainable and clean energy sources. As solar systems become more common, powerful photovoltaic systems still have to be made. The maximum power point (MPP) is this operational point. The PV Panel's power-voltage function is nonlinear and depends on sunlight and ambient temperature. The temperature difference in voltage and power is less important than radiation from the sun.

Since the irradiance from the sun is not constant all day, a PV panel 's performance is not constant either. In addition, the MPP also affects sunlight and ambient temperature as sunlight is changing. Therefore, the conservation of MPP is important in order to achieve full power at any temperature and irradiance. The operating point for a PV panel is called Maximum Power Point Tracking (MPPT) at MPP at any irradiance and temperature.

The management of partial shading is another big problem associated to solar power generation. The radiation of sunlight is not constant over the whole panel under partial shading conditions. A large number of panels are connected for a certain power rating in a PV generation system for a series parley. The panels are subject to non-uniform irradiance under partial shading conditions, and the power-voltage features display several power pits in this situation.

The maximum of this power peak is called Global Power Peak (GPP). A typical power-voltage characteristic of a partial shaded PV system is shown in Figure 1.2. The power output of PV system under partial shading condition is at maximum only when it is operated at GPP. Therefore, under partial shading condition the operating point should be maintained at GPP.

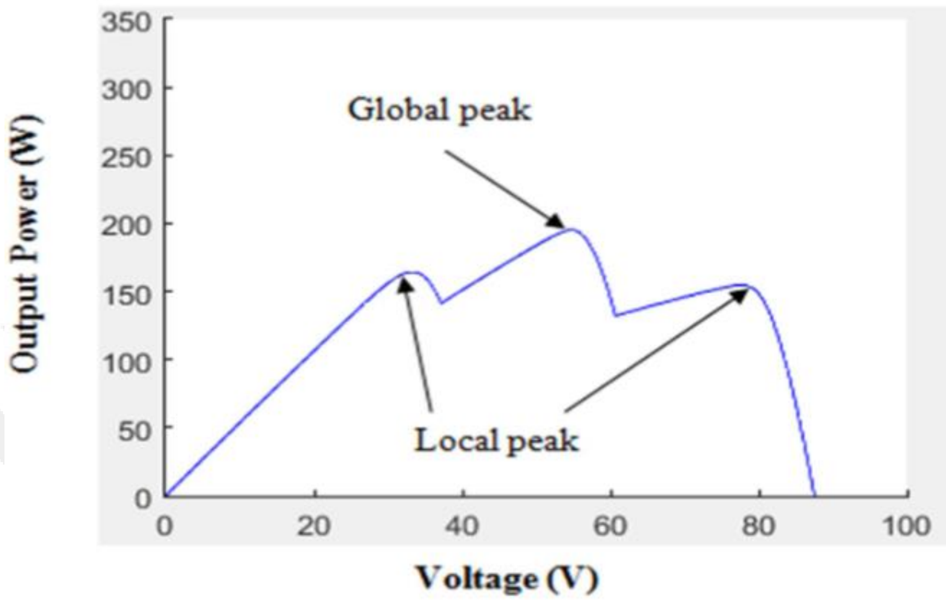

Figure 1.2: Power-Voltage characteristic of PV array under partial shaded condition

1.4 PARTIAL SHADING CONDITIONS

A single MPP with uniform irradiance happens on the power voltage curve as shown in Figure 1.3,

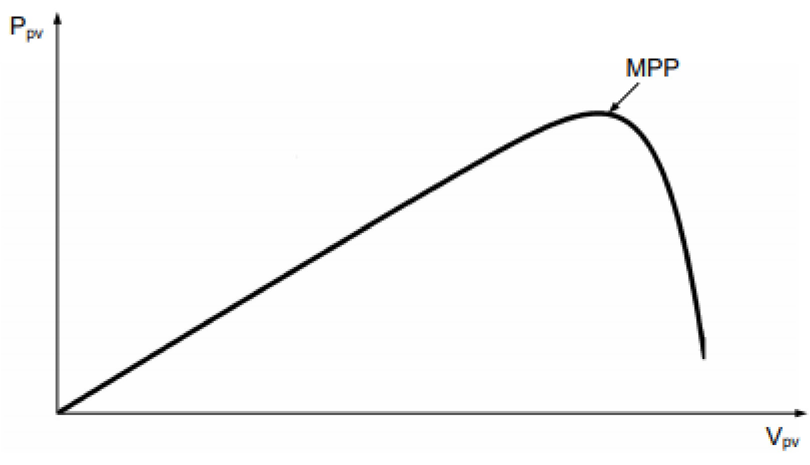

Figure 1.3: Curve of P-V properties with uniform degree of insolation, single MPP**.**

However, when the PV power system receives uneven irradiation, this becomes complicated. If a (or several) module in a solar array is shaded by its voltage, as shown in Figure 1.3 it acts as load rather than generator. (Figure 1.3 shows that the voltage of one module can drop by shading, or by several other factors). Therefore, the development of an MPP-tracker [4] [5] is a challenge for a photovoltaic system. To ensure the specific shaded module is not affected, a Bypass Diode (BD) is attached. Parallel connected modules can cause voltage mismatch.

BD begins to work as shown in figure 1.4 under partial shading (when certain parts of the module are shaded). So, in the P-V curve, as shown in Figure 1.4, we do not get a single MPP, but get multiple local peaks and a global peak. To simplify multiple peak complications BD can be deinstalled from the device. This decreases capacity, which greatly increases solar power production costs.

(a) (b)

Figure 1.4: Shading Examples Possible [4]

Mismatch loss: Mismatch loss (ML) in some situations presents a major problem in the case of photovoltaic modules and arrays, as lowest performance solar cells are the performance of the entire PV module. For example, when the rest of the module is not shaded by a solar module, the energy produced by the good solar module is not powered from a lower electric module rather than dissipated. The resulting local heating may cause the module to dispense with highly located power and irreversible harm. PV modules are primarily divided into two different categories:

Internal ML: Due to changes in the module's physical conditions due to the PV source parameters. External ML: This happens by shifting sunlight, i.e., a partial shading.

$$ML = P_1 - P_2 \quad (1.1)$$

where the insolation level shifts are P1 and P2.

The effect and lack of control because of the incompatibility:

• Operating point of the PV module; • Configuring the circuit; • the different parameter to the solar cell's remaining.

A BD is attached in parallel to a solar cell to avoid this condition, but with opposite polarity. Each solar cell is forward facing under normal operation, so that the BD is reversed to the open circuit. However, the BD offers a current pathway if the solar panel or cell is defective or open. that allows energy to flow to the outside circuit rather than bias any successful cell. A blocking diode is likewise attached to several modules, which are connected to another battery or party, to stop the flow of inverse current. In Figure 1.4 it is clearly seen the value of bypassing and blocking diodes in a PV panel / array and their effect on the PV curve is shown in Figure 1.5.

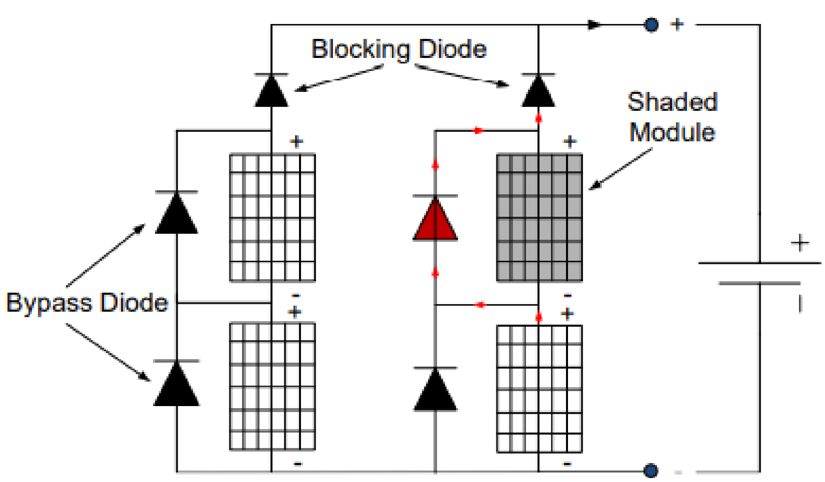

Figure 1.5: Bypass Impact and PSC Blocking Diode.

1.5 BACKGROUND

This study offers a succinct and organized analysis of various MPPT algorithms implemented by PV under Partial Shading (PSC) in the photovoltaic system. Until now several algorithms have been thoroughly explored, including configuration of PV arrays and controller topologies. However, each technology still has its advantages and inconveniences. A correct literature review is therefore important when constructing a partially shaded PV scheme.

The output power of photovoltaics is based on irradiance, temperature, shading and panel environment. PV panels are typically influenced partially or entirely by the clouds, tree shadows, towers and buildings etc. PV panels show a multiple power peak under partial shading condition. To date, it is very difficult to find the global limit under partial shading between multiple power peaks. The proposed study therefore uses meta-heuristic methods to improve monitoring of MPP, which are discussed below.

1.5.1 MPPT Optimization Algorithms

The following literature survey has been carried out to analyze the various optimization techniques and different architectures for PV system to track the best PWM duty for boost converter under partial shading condition.

i) Conventional Methods to Extract Maximum Output Power

In order to monitor the PV panel in the sense of different solar radiations, [6] proposed an improved method for incremental conductance. The key goal was to speed up convergence and also remove the constant state swing.

Dezso Sera et al. (2013) [7] provides a detailed study of two well-known climbing algorithms such as Perturb and Observe (P&O) and Incremental Conductance (INC) for maximum power points monitoring. The dynamic and static conditions are experimentally evaluated according to the EN 50530, and the results suggest that the algorithms are both similar.

Kok Soon Tey et al. (2014) [6] has proposed an improved Photovoltaic Incremental Lead Algorithm to reliably obey the GMPP and thereby to minimize power losses under partial shade and load variance.

Ratna Ika putri et al. (2015) presented Incremental Conductance method using buck-boost converter to reduce the oscillations around MPP compared to P&O algorithm.

Abdelaziz Youcef et al. (2016) [8] formulated a modified P&O to track the global MPP for any shading configuration, irradiation and solved the low irradiation tracking problem of conventional P&O algorithm.

A modified P&O technique was proposed by Bader N. Alajmi et al. (2016) [9] for partially shaded PV systems to identify whether the PV system is under PSC or not. The idea behind the proposed method was to provide accurate and fast convergence to the global MPP during different weather conditions.

Ammar Hussein Mutlag et al. (2016) suggested an enhanced photovoltaic system P&O-based MPPT process. The main aim of this algorithm is to get accurate results compared to conventional P&O algorithm

Alireza Ramyar et al. (2017) [10] proposed a modified Hill Clamping method. The key benefit of this approach is to map the Global Peaks reliably and effectively under different conditions of shading.

Jubaer Ahmed et al. (2017) [10] suggested a partial shading Enhanced Adaptive Perturb and Observe algorithm (EA-P&O). The aim is to mitigate the disadvantages of traditional P&Os such as constant state oscillation, varying tracking path, and failure in partial shading to detect the global peak. The algorithm 's efficiency is evaluated against the artificial colony of bees, adjusted incremental conduction, cuckoo hunt and the P&O-optimizing hybrid ant colony. Results show that the proposed approach effectively monitors the global peak according to various partial shading trends.

ii) Maximum Power Extraction using Meta heuristic Methods

Esmat Rashedi et al. (2009), [12] has suggested a new gravity- and mass-interaction optimization algorithm. The main idea is to improve the performance for various nonlinear functions.

Tat Luat Nguyen et al. (2010) [13] has a direct search algorithm to track the maximum global power point of partially shaded photovoltaic systems. The main aim is to find the GMPP with fast tracking speed.

Ishaque et al. (2011) [14] propose to use the Particle Swarm Optimization (PSO) algorithm to track global MPP in partial shaded conditions. The algorithm proposed for a grid-connected PV system in which both non-shading and shade conditions are efficient followed by the boost (step up) DC-DC converter.

Ishaque et al. (2012) [15] suggest an improved PV system MPPT system the main benefit of this approach Stable state oscillation (to basically nil) should be minimized once the maximum intensity (MPP) is located. The MPP system is assisted by an improved PV system. Moreover, the proposed approach also has the capacity to monitor the MPP for environmental conditions, including varying insolation and partial shading.

Taisir Eldos et al. (2013) [16] implemented a gravitational search algorithm. The objective is fine tuning the algorithm parameters and transition function towards better balance between exploration and exploitation and the results are compared with genetic algorithm.

Jun Sun et al. (2014) [17] proposed a random drift particle swarm optimization technique and used for Hidden Markov Models (HMM) in Multiple Sequence Alignment (MSA). The main aim is to enhance the global search ability of the algorithm.

Mohanty et al. presented a specification for a PV device using the GWO technique (2016) [18]. GWO is a modern optimization approach that removes constraints as in techniques such as low-tracking efficiency P&O and Improved PSO (IPSO) techniques, stable state oscillation and transient. The results obtained showed that the GWO-based MPPT performs better than two others MPPTs.

iii)Maximum Power Extraction using Bio inspired methods

The comparative analysis of two swarm intelligence-based algorithms (FPA and Bat algorithms) has been implemented by Nazmus Sakib et al. (2014). Both algorithms have been able to find the optimal global value of continued optimization problems with swarm intelligence. In terms of final solution consistency, FPA exceeds the Bat Algorithm at most functions. The main cause of the performance discrepancy is the relatively limited number of Bat Algorithm scans for a search space, which could lead to premature convergence around the optimum locals and not to find the world's best spot.

Mohamed Abdel-Baset 2016) [20] proposed a hybrid algorithm called flower pollination simulated annealing to enhance the search performance and to increase the convergence speed.

Jagatheesan et al. (2016) presented a bio-inspired multi-area interconnected power control (LFC) load-frequency control (LFC) Crop pollination algorithm (FPA) tuning Proportional – integral (PID) controller. Tuning algorithm. The Particle Swarm Optimizer (PSO) on a single power system compared to genetic algors (GA) and, the efficiency of the proposed algorithm is calculated the same way.

Proposed a Flowers Pollination Algorithm (FPA) for Prasanth Ram & Rajasekar (2017) [21] in order to find a capacity to achieve global peak. The global and local search algorithm is performed in one step and it is evaluated with zero, weak and strong shading condition. The findings are contrasted with the standard disturbance and observation techniques and Particle Swarm Optimization (PSO) methods and proved that FPA is superior to energy saving methods.

iv)Various PV architecture to extract maximum power

Prague Pradeep S. The differential power processing system architecture was proposed by Shenoy et al. (2012) [22] to improve the output of energy and the dependence of photovoltaic systems. The differential design improves overall conversion performance and tackles the challenges presented by partial shading of unparalleled PAPs.

The comparison between the DMPPT pv system and different topes proposed by Feng Wang et al. (2016) [24]. This paper notes that residential photovoltaic systems are often suffering from power loss, which in real conditions leads to poor results. To increase the efficiency of a PV system in residential usage is important to resolve and minimize PV system power loss under such conditions.

Kyoung-Tak.Kim et al. (2017) [25] Proposed to balance the voltage under partial shading condition a new boost converter topology for a DPP system. The performance of the PV system is analyzed and also hardware model is presented using PSIM.

1.5.2 Hybridization MPPT Algorithms

This section demonstrates the significance of hybrid MPPT algorithms for MPP Tracking under partial shading compared to traditional MPPT algorithms.

The new hybrid population-based Algorithm Seyedali Mirjalili et al (ICCIA 2010) [26] proposed that PSO's exploitable capability should be integrated with GSA explorative capability. The results show that the proposed hybrid algorithm can escape the local optimum with faster convergence than the PSO and GSA norm.

Lian et al. (2014) [27] addressed the PSO method problematic, namely that if the scope of the search is broad, the time needed for convergence can be long. A hybrid approach that combines P&O and PSO approaches is proposed in this paper. The first step is to assign the local limit of the P&O system. Then the PSO approach is used to check for GMP starting from that point forward. The benefit of using the proposed hybrid approach is a reduction in PSO search space and thus substantially improved time required for convergence.

Lyden & Haque (2015) introduces the photovoltaic (PV) hybrid MPPT device that has standardized environmental or partial shade conditions. This approach is used to trace maximum power point. Two simple strategies combine the hybrid approach with additional intensity in order to achieve a global MPPT. The global maximum with minimal implementation complexity is calculated by Simulated Annealing (SA), and the MPP is controlled in continuous Perturb and Observe (P&O). By combining these techniques with a hybrid MPPT approach consisting of a global search and a local searching level, the tracking process is enhanced.

The hybrid algorithm was proposed by Jie-Sheng Wang et al. [12] to solve function optimization problems, to improve the convergence rate and to improve the accuracy of the solution.

1.6 MOTIVATION OF RESEARCH WORK

In particular, three factors are involved in the success of a photovoltaic power station: the conversion efficiency of the photovoltaic plate, the effectiveness of the converter and the MPP monitoring by algorithm. It is not easy to boost the performance of the PV panel and inverter, as the available technologies will mean that better elements are required that can dramatically increase installation costs.

It is, however, simple and not costly to improve the monitoring of MPP with efficient control algorithms, even in plants that have already been used by the upgrade of their control algorithms, resulting in immediate increases in PV power generation and thus a decrease in its price. In this regard, the utilization of optimization algorithms to track the MPP of PV panels leads to a stabilized and highly efficient PV power system. It reduces the price and complexity of installing high end electronics to track the solar power and leads to a better utilization of solar power.

This has motivated the present study to use optimization algorithms to create a new optimal MPP system. The utilization of such optimization process can lead to an economical PV system. Further, the system can be modified easily and can be implemented in both rural and urban areas. By creating an optimal tracking of the sun, the solar power is readily made available for the user and the affordability is higher than conventional energy system.

• The stochastically differing shadow pattern calculates global MPPs, and the PV modules are configured into PV arrays. Given the stochastic nature of solar radiance in the process of controlling the global MPP, global MPPT algorithms should be implemented.

• Therefore, an appropriate evolutionary calculation technique can be used to resolve the above optimization issue.

1.7 PROBLEMATIC STATEMENT

Take into account the power-voltage characteristics of a PV array that has many shading conditions, More nuanced in a range of local and global MPPs. This situation therefore differs greatly from the case of uniform solar irradiances, where only one MPP is available. With this in mind, the global MPP needs to be calculated. To find the global MPP using different optimization techniques to maximize power extraction under a uniform photovoltaic solar radiation, the MPPT algorithm must be built.

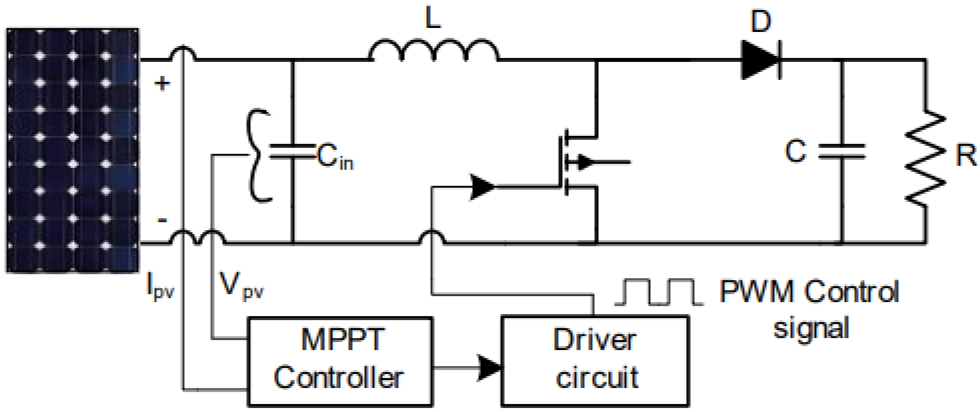

Figure 1.6: A PV system with MPPT

Figure 1.6 displays the proposed scheme topology in which G stands for W / m2, and T is absolute, Vpv and Ipv are the voltage and actual PV arrays respectively. Global optimization problems are induced by global MPPT algorithms with the MPPT control problem when solar irradiation is not consistent.

The goal here is to optimize PV arrays' power extraction from PSCs. The problem of optimization is as follows. Let Np wolves have a solution vector of duty cycles:

$$x_k^i = d_g = [d_1, d_2, \ldots, d_j] \tag{1.2}$$

Although j=1, .. Np, d are the duration of service, I are the current gray wolves.

The objective function is defined as

$$P(d_k^j) > P(d_i^{k-1}) \tag{1.3}$$

Where P = V — the operating power of the PV array for the issue is for any instant.

1.8 OBJECTIVES OF RESEARCH WORK

The main objectives of this research are to determine the best PV optimization algorithm for part shading, by selecting the optimum PWM duty value for the boost converter with high performance, fast response and high efficiency. theme of the research is.

The specific objectives is To attain maximum output power, higher efficiency and faster convergence under partial shading condition by employing different PV power processing architecture such as central, string and Differential Power Processing (DPP) architecture along with optimization technique called Grey Wolf Optimization (GWO) algorithm and comparing the simulation results with PSO and RDPSO algorithms.

1.9 CONTRIBUTION

In the various available renewable energy sources, Photovoltaic (PV) energy has many advantages such as pollution free, easy to maintain, absence of gas emission and no fuel cost. The reduced power output of the PV system is due to the environment such as irradiation and temperature fluctuations and partial irradiation shading. The PV panels will deliver maximum power output only at a certain load voltage and current. The PV panel shall work on the Maximum Power Point (MPP) and create the condition called maximum power point tracking (MPPT) in order to extract maximum power from the panel irrespective of the environmental and load variations.

Partial shading of irradiation is mainly due to shadows of trees, buildings and towers, passing clouds and dust. Under Partial Shading Condition (PSC), the PV array exhibits local power peaks corresponding to individual PV panel and a Global Power Peak (GPP) for the overall series-parallel combination of PV panels. Therefore, under PSC the GPP point has to be tracked to achieve MPPT. Tracking GPP is the main challenge under partial shading condition. To overcome these issues, optimization techniques are used to track the GPP.

The GWO MPPT and P&O MPPT for maximum power for a PV system featuring different models are also included to scale up GWO's search space to accelerate convergence to GP. An experimental configuration of the 600W solar simulator is used in a laboratory with features of partial shadows. In the first case, the algorithms for a PV system were implemented with MATLAB / SIMULINK. The above experimental configuration is then used to implement the MPPT algorithms globally proposed. The simulation and the experiments show that the MPPT converging allows maximum power from a solar photovoltaic device with minimum time.

In this study, theoretical modelling of PV modules is carried out for the handling of non-uniform radiation as well as the development of a new PV modulus RP design for maximum power and fill factor. Two new MPPT algorithms, namely MPPT (GWO-MPPT) and PO (GWO-PO), To obtain the maximum power from non-sunny solar irradiation panels have been built.

In this study, theoretical modelling of PV modules is carried out for the handling of non-uniform radiation as well as the development of a new PV modulus RP design for maximum power and fill factor. Two new MPPT algorithms, namely MPPT (GWO-MPPT) and PO (GWO-PO), To obtain the maximum power from non-sunny solar irradiation panels have been built.

1.10THESIS OUTLINE

The thesis organization is summarized as below:

A general overview about the PV system and MPPT algorithm solution are presented in the second Chapter.

Chapter 3 deals with the analysis of PV array under partial shading condition by employing different PV power processing architecture such as central, string and Differential Power Processing (DPP) architecture for boost converter and with MPP optimization by Grey Wolf Optimization (GWO) algorithm and comparing results with PSO and RDPSO. The DPP architecture and the GWO algorithm led to greater efficiency for monitoring is observed, output power and faster convergence.

Chapter 4 highlights the conclusions and possible future works. It concludes that the DPP architecture with GWO algorithm is the best suited one for PSC. The suggested extension of research work is the study of PV system with PSC connected to standalone load via inverter.

2. LITERATURE REVIEW

The output energy of a given photovoltaic configuration system could have been adjusted according to external parameters such as temperature, irradiation, wind and humidity. The two first parameters of the PV control system design are the main one.

This fluctuation in energy is seen in the PV array power curve and can change its form in various ways, by shifting the MPP bound to the power converter 's working cycle. Once this MPP is relocated, the power point is no longer extracted and a set of MPPT control algorithms have been developed over the past decades to counter this problem.

These MPPT techniques can be divided by group based on its features, such as the control variable and the converter, accuracy, performance, application and algorithm category. In the following sections, their classes of algorithms are described in most popular and actual MPP techniques, which are: traditional (deterministic), soft (stochastic) and other (unusual) algorithms. The following techniques are described by.

2.1 PHOTOVOLTAIC SYSTEM

The main architecture of the proposed PV system is shown in Figure.2.1. A PV power extractor, a Boost converter, a lower load controller and an MPPT controller are included in the module. Displays the respective solar cell type two-diode circuit. The model contains the current source of Iph, two d1, d2 and several resistors for Rs and Rp. Id1 is the reverse saturated current where Ip is its pv current, RS and Rp is the series and parallel resistance equivalent. The PV module characteristics are modelled using the two sample diodes. This is known to have better precision at the low irradiation stage, which enables a more precise forecast of PV system output in partial shading (PS) conditions.

Cells can turn solar energy into electricity, or photovoltaic energy. In this respect, the material they are made of depends on the photoelectric effect, which means that they will emit electrons while the photon beam irradiates his region of the photoelectric material.

In the above-mentioned property, the typical material used in cell production is silicone, a well-known semiconductor that has a mixed form of properties found in the material metal and insulation, allowing photoelectric effect phenomena.

The configuration of the material is based essentially on the same diode application. It consists of a p-n link comprising two separate layers, each of which has been doped differently. The positive side is n-type. Since doped in the last valence layer, usually phosphorus, with a molecule containing more than four electrons, the combination produces an additional "free" electron. In the other hand, the p type layer is used for other forms of doping where the doping molecule has fewer than four electrons in the last valence layer and, in this case, leaves a 'holes.

Thus, in the junction field, freelancing electrons occupied holes, while the n-type area was positive by the loss of freelancers and the p-type zone was negative by the loss of the holes, the two-layer cross-connection formed a region known as the depletion layer. This depletion layer is then already established, and a slightly electric field is produced between the two sides which prevents the movement from freer electrons from an area of n type into a region of p type [18].

Finally, additional energy coming from the photons into the depletion layer is needed to produce current. If this energy is sufficient to overcome the bandgap threshold, an electron-hole pair that is separated by the electric field that exists between the two strata will be produced. When the circuit is closed, electrons will pass through it to produce a continuous current (Figure 2.1)

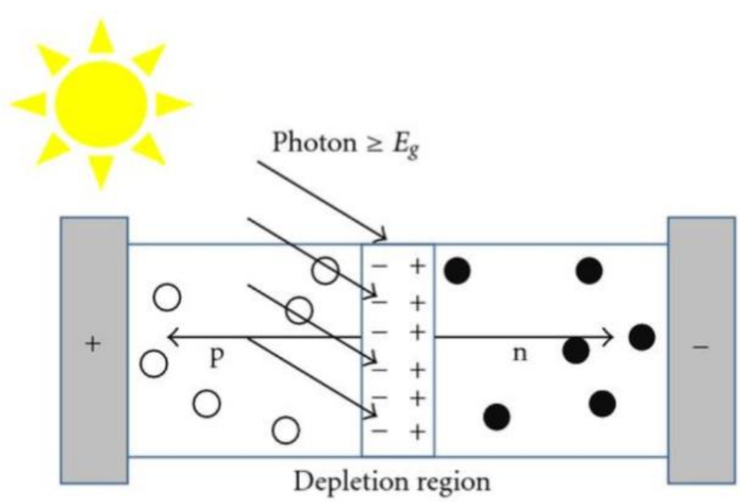

Figure 2.1: p-n junction

While silicone technology is the most common, and it continues to be used even more, as technologies develop in this period, there are other technology and numerous ways to cope with materials. CdTe and CIGS, which have actually enhanced their effectiveness to process solar energy at the same level (and at silicone cell level) in the last 50 years, nevertheless account for less than 10% of the total material used in cell manufacture (from 5% to around 20% in all cases). [19], (Figure 2.2)

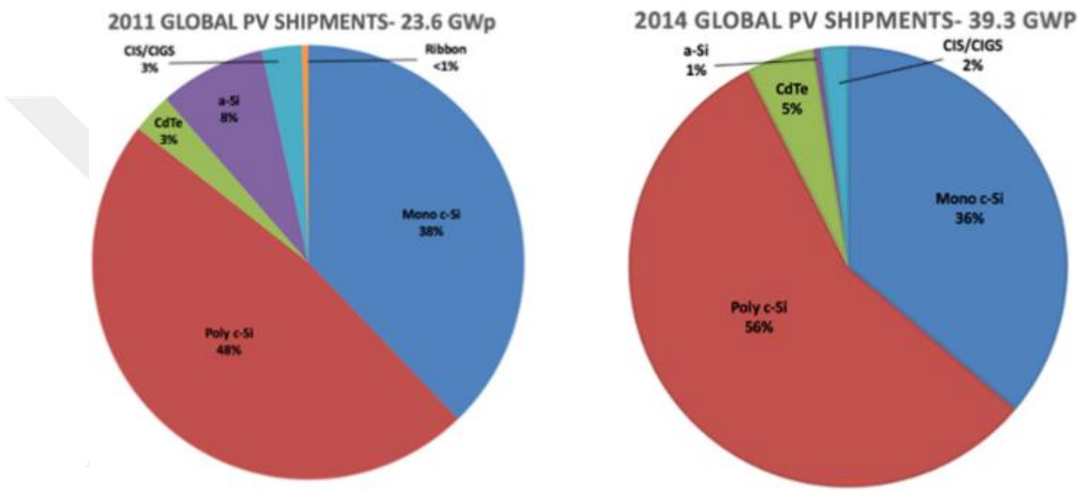

Figure 2.2: Cell fabrication materials

2.1.1 PV Output Characteristics and Models

2.1.1.1 PV Output Characteristics

In order to display the outputs of PV performance characteristics [30, 29], P V and I-V curves typically are used. In general, the PV output properties are shown under five key parameters, including Voc, Isc, MPP Vmpp, MPPimpp voltage and MPP. Voc is the most widely used format for MPP power as shown in Figure 2.3.

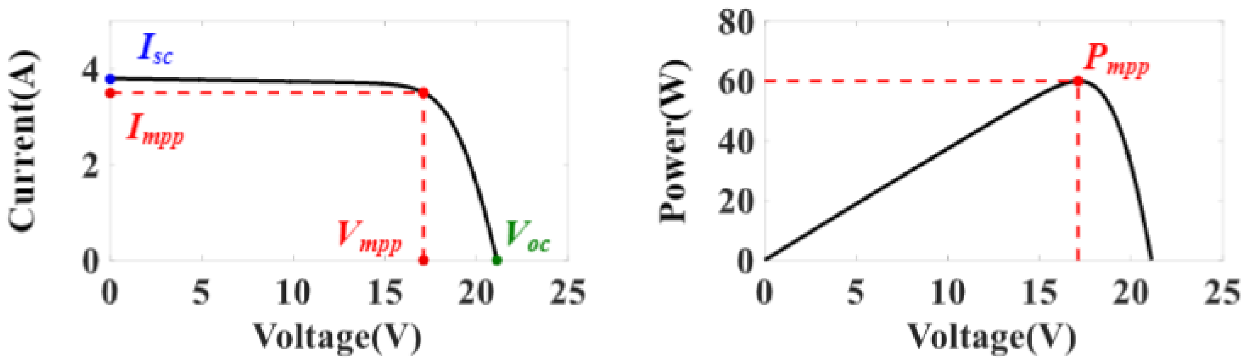

Figure 2.3: Five key PV performance function parameters.

These parameters are normally given in the standard test conditions (STC) of PV manufacturing data sheets where the solar radiance is1000W / m2 and the cell temperature is25 megabyte. The Solarex MSX-60W is selected in this paper and its electrical features are presented in Table 2.1.

In order to derive PV characteristics in different weather conditions, apart from the five key parameters Also important are the above mentioned Kv open circuit voltage temperature coefficients and Ki short circuit power. The heavy dependency on the photovoltaic power outputs on different temperatures and solar radiation levels is shown in Figure 2.4[30]. The temperature affects Voc greatly but does not have a major effect on Isc. Meanwhile, Voices' logarithmic dependence on solar and Isc's dependence on the irradiance is linear. An equivalent circuit model and related equations are needed for the analysis of the behavior of the PV output characteristics.

2.1.1.2 PV Equivalent Circuit Models

Typically, the PV cells or PV modules are represented by an analogous circuit model. In previous research [31], The single model (SDM) of the diode has frequently been used. As Figure 2.4 shows, the SDM models transmit current voltage (I-V) characteristics:

$$I_{pv} = I_{ph} - I_d - \frac{V_d}{R_p} \qquad (2.1)$$

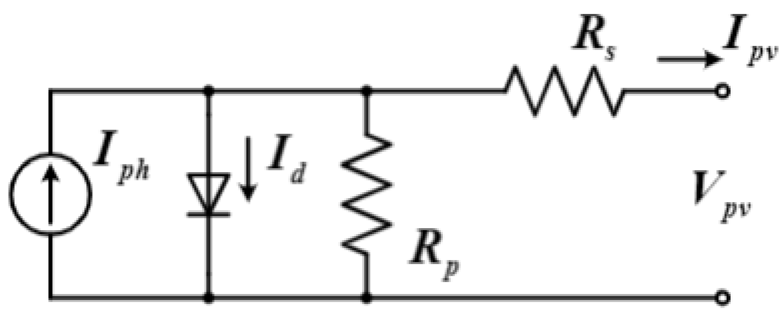

Figure 2.4: Single-diode model (SDM) equivalent circuit.

If Iph displays a photon present, Id is the diode equation of Shockley, which is expressible as:

$$I_d = I_s\left[e^{\frac{v_d}{\eta v_t}} - 1\right] \tag{2.2}$$

Where is the reverse diode saturation and μ is the ideality factor of the diode? Vd and Vt are talking about:

$$V_d = V_{pv} + I_{pv}R_s \tag{2.3}$$

$$V_t = \frac{KT}{q} \tag{2.4}$$

Where Vt 's thermal voltage, k is a constant Boltzmann (1.38 to 10−23J / K) T, (in Kelvin), the electron charge (1.602 to 10−19C) is the p – n junction temperature. It can be substituted as (2.2-2.4) in (2.1):

$$I_{PV} = I_{ph} - I_s\left[e^{\frac{v_{pv}+I_{pv}R_S}{\eta V_t}-1}\right] - \frac{V_{pv}+I_{pv}R_S}{R_p} \tag{2.5}$$

The 5 PV parameter model is known also as the SDM as five parameters are unknown (2,5) [25].

Many techniques for the parameter estimation were proposed and tested in [32] in order to achieve these unknown parameters. This work is based on the model of Device Advisor of the National Renewable Energy Laboratory (NREL). Therefore, based on the NREL Device Advisor

Model, Table 2.1 obtains five unknown parameters. Table 2.1 displays the obtained values for five STC parameters.

This thesis assumes constant parameters μ, Rp and R when weather conditions are modified [33]. If and is expressed as different solar irradiance and temperature:

$$I_{ph} = \left[I_{ph,STC} + K_i(T - T_{STC})\right]\frac{G}{G_{STC}} \tag{2.6}$$

$$I_s = I_{s,STC}\left(\frac{T_{STC}}{T}\right)^3 e^{\frac{qE_g}{\eta K}\left(\frac{1}{T_{STC}} - \frac{1}{T}\right)} \tag{2.7}$$

When G and T apply to solar irradiance values, GSTC and TSTC refer to the value of the solar irradiance and temperature of the STC; Iph, STC, and Is, STC refer to Iph and Is at STC; e.g. the semi-conductive bandgap energy (e.g.= 1.12eV for poly-crystalline Si at25).

Table 2.1: Five criteria based on the Model System Advisor System for National Renewable Energy Laboratory (NREL).

Parameter	Variable	Value at the STC
Photon current	I_{ph}	3.8091A
Diode saturation current	I_s	2.452e^{-10}A
Reverse ideality factor	η	0.97359
Parallel resistance	R_p	161.0752Ω
Series resistance	R_s	0.38659Ω

2.2 MPPT INTRODUCTION

2.2.1 MPPT Operating Principle

Impedance between the output of the PV generator and the load conditions is the theory behind MPPT [24]. Providing a direct connection of a PV panel with a load for resistance as shown in figure 2.5 (a). If the resistance is 7.61 dc, A crossing point between the I-V curve and the load-axis is the operating point. By changing the value of the resistor shown in figure2.5(b), the operating point will change the PV I – V Curve itself, if connected to the variable resistor module.

The load typically requires a constant current or a voltage, such that the load impedance for the MPPT cannot always be changed. An updated interface is thus linked to the same MPP intensity between the PV generator and load as shown in Figure 2.6. Suppose that the DC-DC is a controlled control interface with input and voltage, and with input and voltage respectively; source and control output voltage are power output and voltage; d is the duty cycle of the DC-DC converter.

If the DC-DC converter is sufficient, the mathematical expression may be used.:

$$V_{in} = \frac{V_{out}}{M(d)} \tag{2.8}$$

$$I_{in} = M(d) \cdot I_{out} \tag{2.9}$$

The voltage conversion ratio is where M(d) is. It can be extracted as a division (2.8) by (2.9):

$$R_{in} = \frac{V_{in}}{I_{in}} = \frac{V_{out}/M(d)}{M(d) \cdot I_{out}} = \frac{1}{M(d)^2} \cdot \frac{V_{out}}{I_{out}} = \frac{R_{out}}{M(d)^2} \tag{2.10}$$

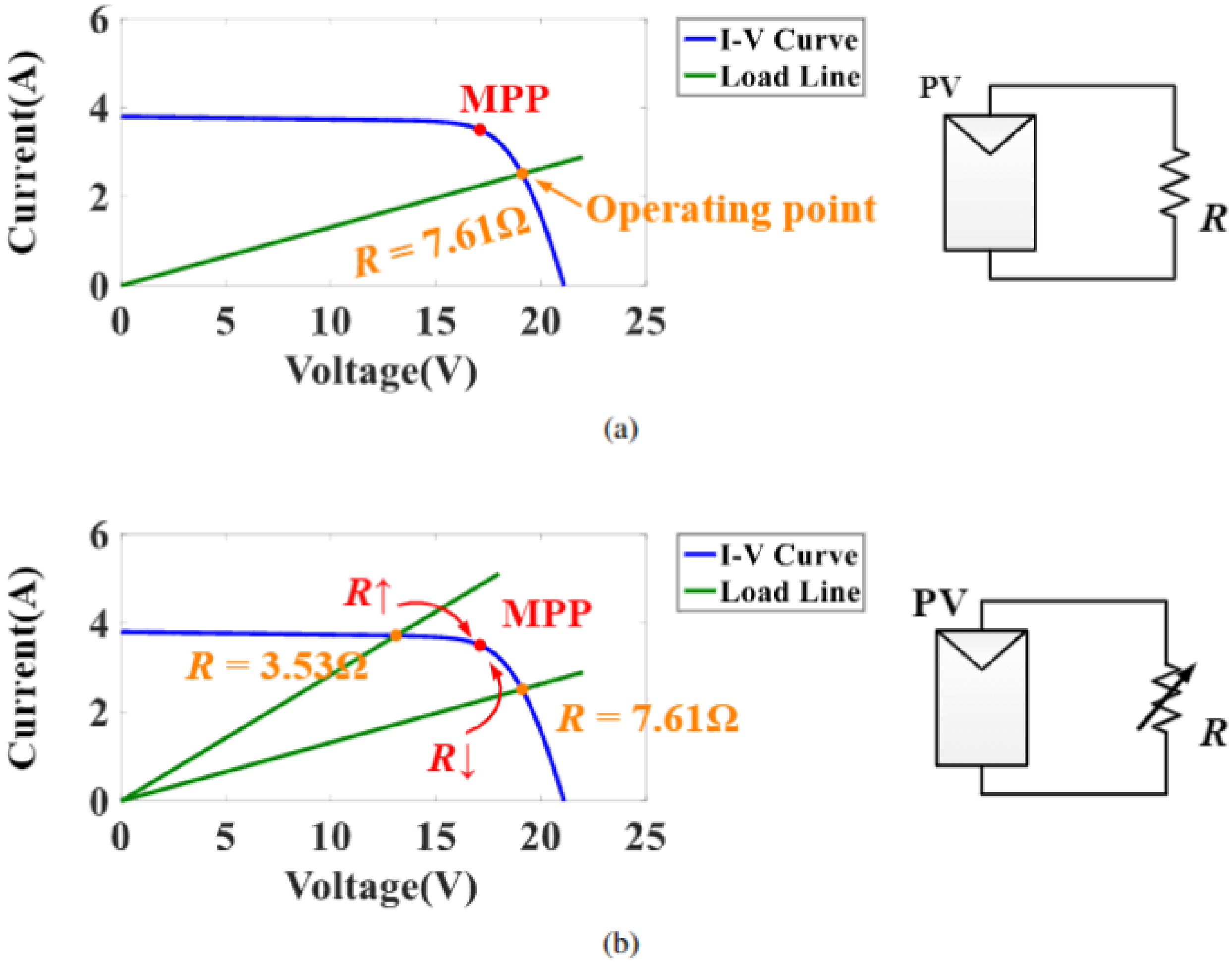

Figure 2.5: Impedance of MPPT: (a) load match direct; (b) load match vector.

Where Rin is the resistance of the input and Rout is the resistance of the output. The PV source is the DC-DC input, so (2.10) can be rewritten as PV source:

$$R_{pv} = \frac{R_{load}}{M(d)^2} \tag{2.11}$$

Where Rpv corresponds to the corresponding PV source resistance, the load resistance represents Rpv. Note that for various DC-DC converters there is different M(d), as summed up in Table 2.2 take as an example the boost converter displays its M(d) as follows:

$$M(d) = \frac{1}{1-d} \tag{2.12}$$

Substitute (2.12) into (2.11), it can be derived as:

$$R_{pv} = R_{load}(1-d)^2 \tag{2.13}$$

The left terms (2.13) can be viewed as equal resistance from the discussion above. This is shown in Figure 2.6 with the corresponding I-D-V curve., provided the boost is used and the charge is set to 25 lbs. The operating point alone can be adjusted by changing the value of d to the PVI-V curve.

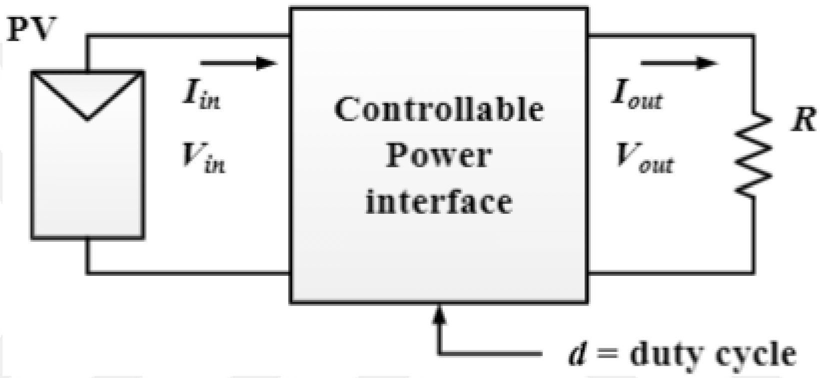

Figure 2.6: Regulated power interface between PV and load generator.

Table 2.2: DC-DC converter summarizing of M(d) and Rpv.

Converter	$M(d)$	R_{pv}
Buck	d	$\frac{1}{d^2}R_{load}$
Boost	$\frac{1}{1-d}$	$(1-d)^2 R_{load}$
Buck-Boost	$-\frac{d}{1-d}$	$\frac{(1-d)^2}{d^2}R_{load}$
Cuk	$-\frac{d}{1-d}$	$\frac{(1-d)^2}{d^2}R_{load}$
SEPIC	$\frac{d}{1-d}$	$\frac{(1-d)^2}{d^2}R_{load}$

2.2.2 MPPT Categorization Base on Algorithmic Characteristics

In terms of the success of the MPPT methods, two points must usually be taken into account [34], that is to say, the efficiency of the steady-state MPPT methods and the efficiency of the dynamic MPPT, when the weather conditions do not change, is to be seen as the efficiency of the MPPT methods. The MPP is often used to define the precise location of the MPP since the operational point is around the MPP during the stage of stable control. In general, MPPT stability is expected to be high in efficiency (typically above 99%).

The MPP must be moved, and this step is called dynastic stage if weather conditions are changed. The efficiency of MPPT methods shows how easily the MPP is pushed during the dynamic process. The complex efficiency of MPPT may be more than 98 percent, based on previous studies. [10].

In the literature [35] a significant number of MPPTs have so far been suggested. The properties of the available MPPT can be roughly divided into three categories.

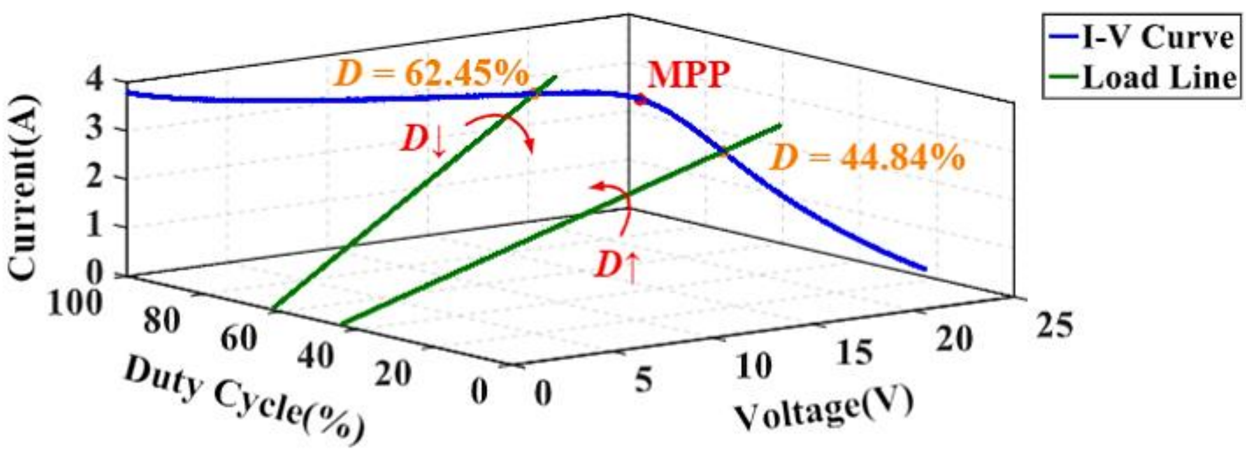

Figure 2.7: D – V impedance curve for regulated interface power.

The heurism process is based on the trial-and-error approach [36, 37]. First of all, the algorithm disturbs the PV system. The algorithm then tracks and takes appropriate action on the effect caused by this disruption. This method is repeated until the best point is reached. In general, under different weather conditions, the heuristic method is relatively simple and very efficient.

However, its low performance under rapidly changing weather conditions is the downside of such algorithms [37].

The models are based on the MPP model [38] of the PV generator, there is also generally better than heuristic the dynamic performance of this algorithm., and it can be calculated by these algorithms. However, PV model accuracy affects the efficacy of the model-based procedure.

The hybrid approach incorporates the heuristic method with the modeling method, which takes advantage of its advantages and overcomes its disadvantages. [28, 22]. The hybrid approach typically has two phases. The model-based approach is used to dynamically estimate the MPP climate. The heuristic method is used to find the exact MPP when the dynamic process has shifted to the static level.

2.2.3 MPPT Categorization Base on MPPT Implementation

The MPPT processes can also be classified into five classes, as shown in Figure 2.8, based on MPPT implementation, except for algorithmic characteristics. The current and/or voltage sensor of the PV side is needed for figure 2.8(a). The most common implementation. It should be noted that this implementation is the basis for the majority of the MPPT methods available [15]. In comparison, as shown in Figure 2.8(b), A captive output voltage and/or current capture for the generation of MPPT may also be used. But this kind of implementation cannot be guaranteed by true MPPT [15].

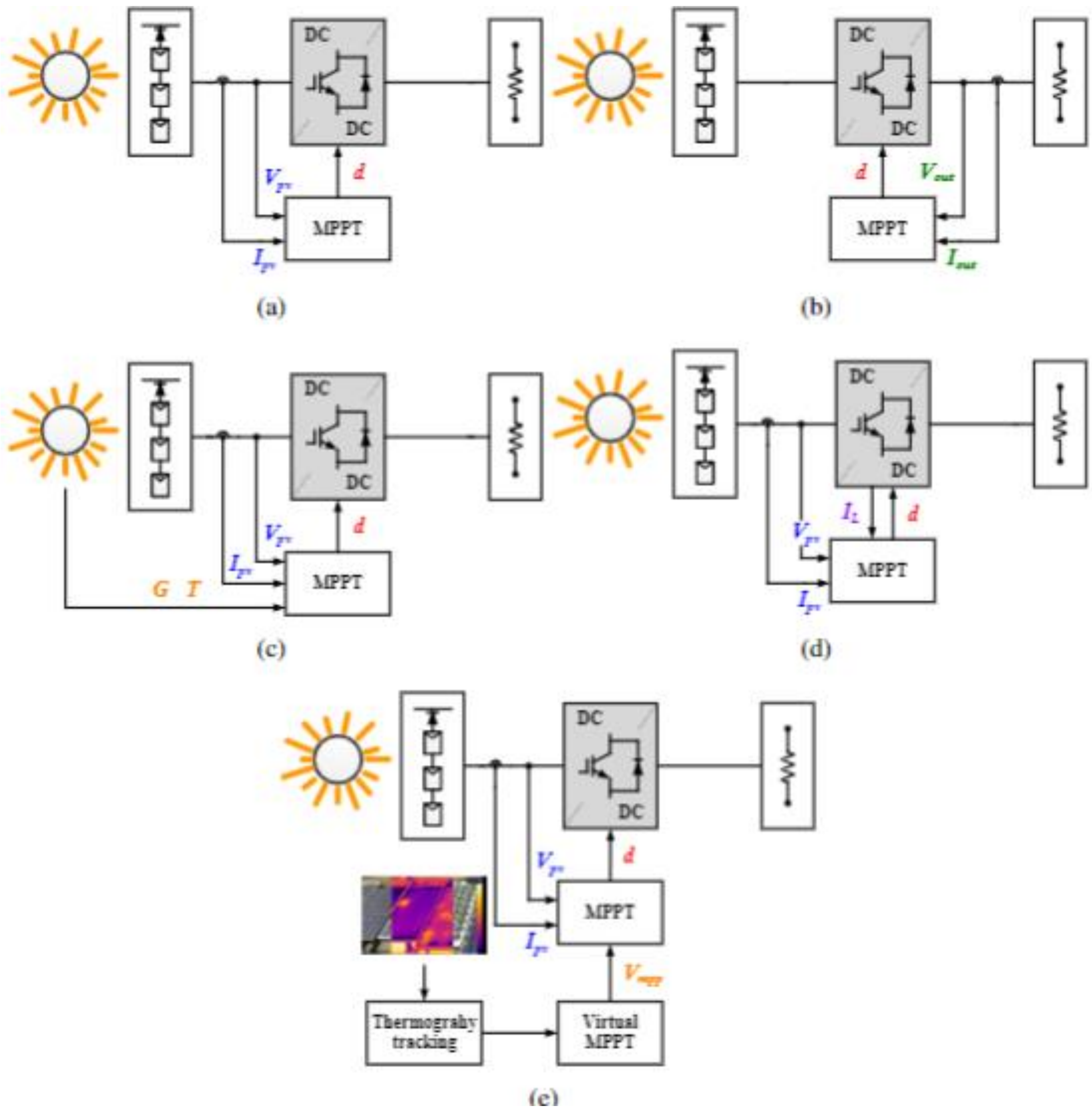

Figure 2.8: The various implementations of MPPT are: (a) PV-side sensors; (b) output sensors; (c) additional solar radiance and/or temperature sensors.

In certain MPPT implementations, additional sensors are also used. Solar irradiance and/or temperature are as shown in Figure 2.8(c) and transmitted to the MPPT controller. Overall, this implementation is also necessary only for model-based methods and some MPPT methods [31]. In addition, a certain MPPT approach involves measuring current of the inductor as shown in Figure 2,7(d), such as sliding mode (SM) control [39]. In recent years, thermographic virtual MPPT [40] has been proposed to be used for MPPT with the aid of a thermographic camera,

Figure 2.8(e) indicates this. Although additional sensors confirm the efficiency of these systems, costs and complexity are generally great since more sensors are used.

2.3 MPPT TECHNIQUES FOR PARTIAL SHADING EFFECTS MITIGATION

MPPT traditional algorithms typically use one or more electrical parameters to compare the system values produced by the sensors in certain electrical features of the energy system. This measures the error of the closed loop control system and makes the necessary corrections.

Stochastic algorithms use several time steps to set values and to apply the corrections to the algorithm, before the method reaches the convergence point, to create the next family of the value.

It is normal to find system work MPP in the whole package of algorithm forms, and therefore achieve the maximum possible efficiency of the system as a whole.

2.3.1 Deterministic MPPT algorithms

This type of algorithm is based primarily on the concept of a simple cause and effect. In most instances, it uses a comparison of two stages to evaluate effectively how the mechanism responds to the algorithm following application of a disturbance and then behaves in consequence.

Literature is generally consistent with the fact that this type of algorithm has a sufficient output in those cases where there is a unique maximum of the power curve which represents the PV array configuration, or, in other words, in which irradiation is constant and homogenous in the entire PV area.

2.3.1.1 Perturb and Observe and incremental conductance method

Perturb and observation (P&O) and incremental conductance (INC) are the most important hurt approach. Figure summarizes the operating theory of the P&O system and of the INC. [41]. 2.8. The direction of disturbance and disturbance must be calculated both by the P&O method and the INC method from Figure 2.9. [42].

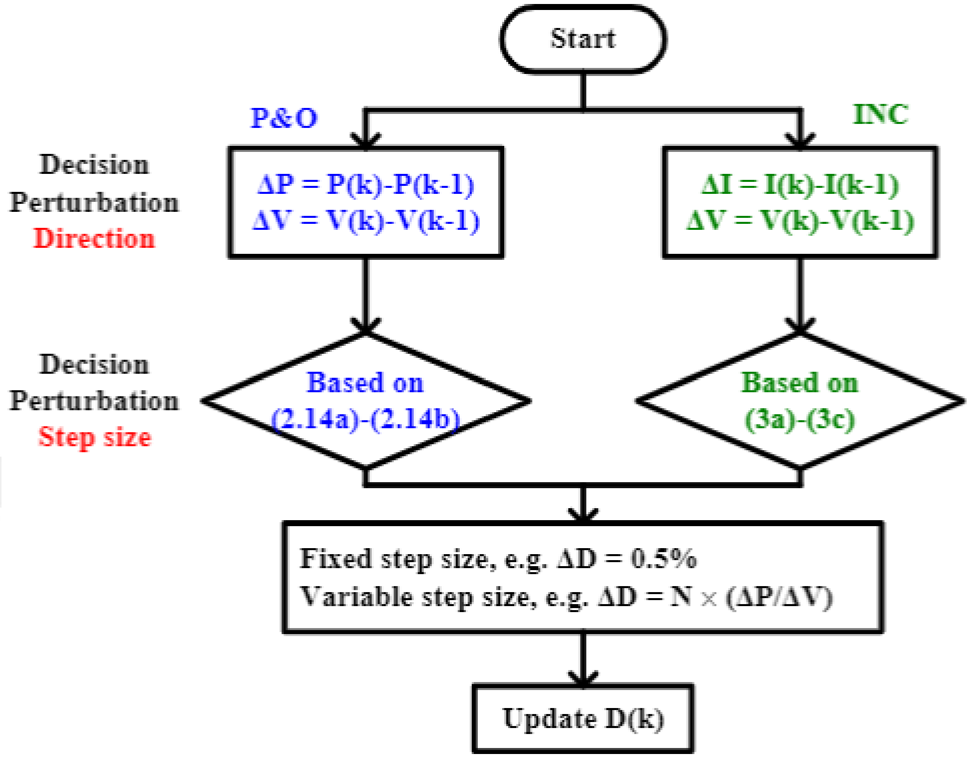

Figure 2.9: The P&O and INC approaches summarized flow charts.

Figure 2.10 demonstrates the direction of perturbation for P&O and INC methods. P&O and INC derive from P-V features, as shown in Figure 2.10 that could be summarized as a disturbance route:

$$P\&Of(x) = \begin{cases} \frac{\Delta P}{\Delta V}, & > 0, left\ of\ MPP \\ \frac{\Delta P}{\Delta V}, & < 0, Right\ of\ MPP \end{cases} \tag{2.14}$$

$$P\&Of(x) = \begin{cases} \frac{\Delta I}{\Delta V}, & > -\frac{I}{V}, left\ of\ MPP \\ \frac{\Delta I}{\Delta V}, & = -\frac{I}{V}, At\ MPP \\ \frac{\Delta I}{\Delta V}, & < -\frac{I}{V}, Right\ of\ MPP \end{cases} \tag{2.15}$$

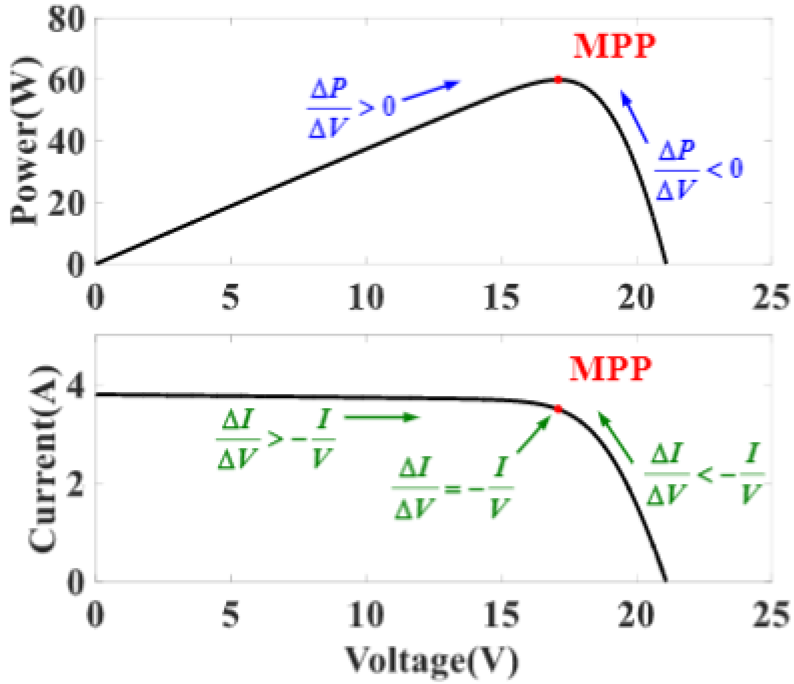

Figure 2.10: Determination of the P&O system and INC system disturbance path.

Figure 2.11 illustrates the work of the INC and P&O approaches in a stable state. The A and C shall apply on the left of the MPP and on the right of the MPP. Point B applies to almost the same spot as the MPP. The point A to point B (2.14a) and (2.15a) is fulfilled if the working point is shifted. Thus, the point of action begins to travel to the right and hits C. The operating point is reached at C (2.14b) and (2.15c), so it is returned to B. The operating point then begins to turn to the left (2.14b) and (2.15c). Finally, this operating point will replicate this phase after the trajectory (A) in the current state (B) in the current state(B) in the case of (B) to(B) in the current state(A) [35]

These two methods will typically step correctly towards the MPP. In most cases. But such methods can lead to incorrect motion and a sudden increase in solar irradiance [10] from the MPP. The operating point's movements under sudden irradiance variations are shown in Figure 2.12. if suddenly the solar radiation.

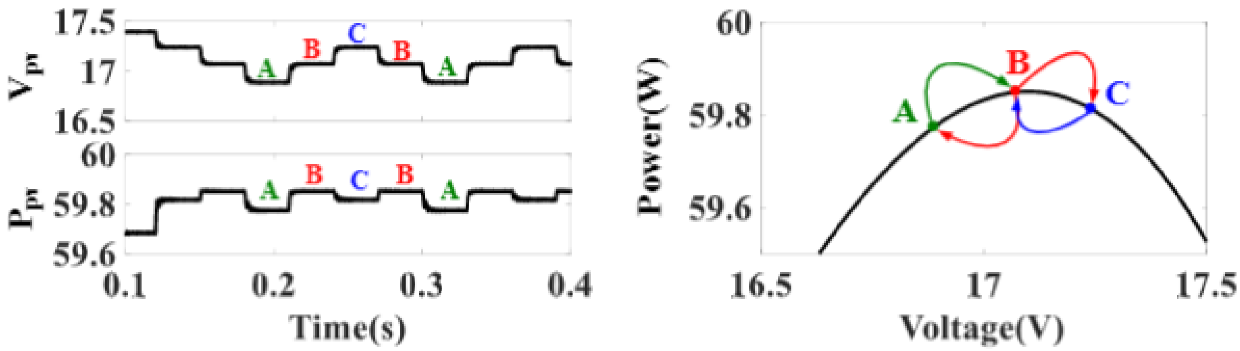

Figure 2.11: Three-level steady-state swings around the MPP.

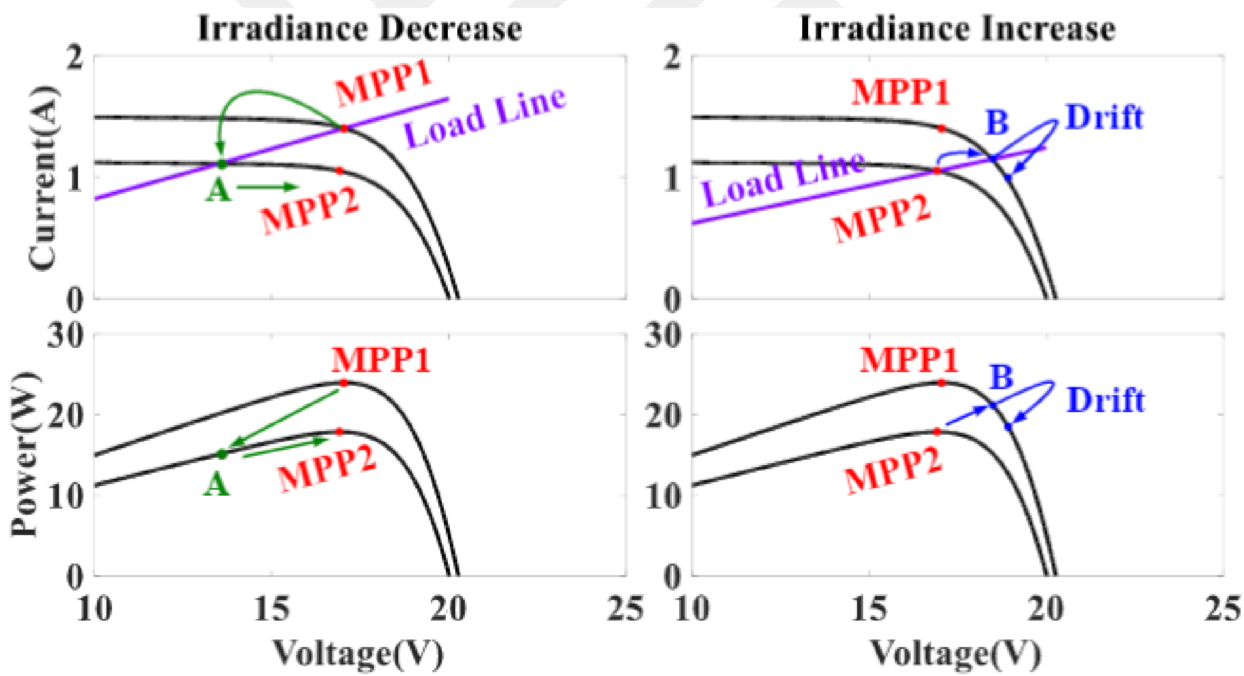

Figure 2.12: Operating point movements under the abrupt shifts of irradiance.

The operating point therefore moves immediately through the loading line from MPP1 to A. As ΔP, ΔV and ΔI are reduced at this point, these are (2.14a) and (2.15a) respectively. The INC and P&O method move to MPP2 correctly and there is no drift. If the solar irradiance increases abruptly, the operating point switches automatically from MPP2 to B. Nevertheless, the quantities − asset, assignment V, and assignment I are increased and (2.14a) and (2.15a). The P&O and INC systems and the operating point are so far separated from the MPP1. In the methods P&O and INC, the fixed-stage scale is commonly used for disturbance phase dimensions [35]. At the same time, though, continuous performance optimization and dynamic performance is very difficult. [10]. The various fixed-stage sizes of the P&O and INC system are illustrated by Figure 2.13. Providing that the MPP is monitored at the same starting point with two separate phases, i.e., 1V and 0.5V. The larger stage approach with better dynamic efficiency can be seen from Figure 2.13. In order to achieve the MPP, the larger method requires only 6 steps; the smaller step requires 11. When the MPP is hit, the unit will swing around the MPP. This results in better steady state performance of the system with a smaller phase scale. As a previous discussion, the fundamental P&O and INC approaches have three disadvantages:

• Drift conditions under abrupt radiation changes • Simultaneous optimization of steady state output and dynamic output •Steady state oscillations at a constant state point.

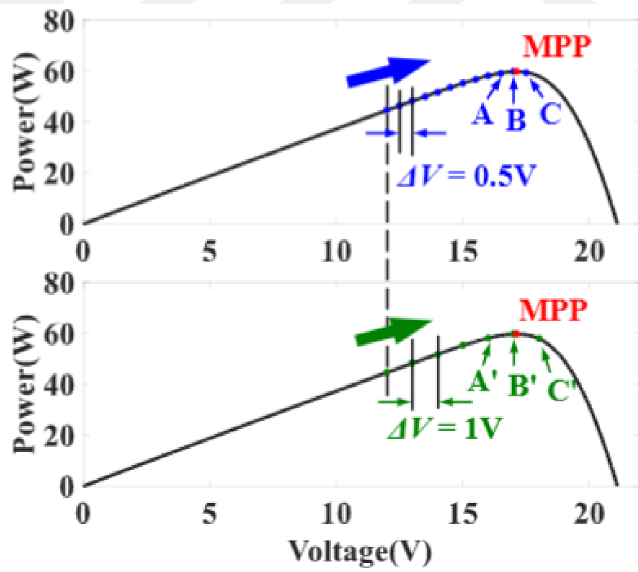

Figure 2.13: Performance of various P&O and INC fixed stage sizes.

2.3.2 Stochastic MPPT algorithms

There have been identified some traditional MPPT algorithms. They have the enormous advantage of finding an optimal global of their necessary function in a standard deterministic algorithm method from this family. Unfortunately, the multiple local maximum features give the tracking system a problem that is typically not prepared for this type of algorithm.

A complex power curve shape will be produced that contains one or several maximums depending on the situation, set-up configuration, and partial shading conditions. The previously implemented control techniques would therefore be able to fail in the mission to define and obey the optimum electric relation involving the photovoltaic system's maximum extracted power. If the selected point is not ideal, the device will experience a high reduction in power extracted that means low efficiency and a lower return on inversion after a number of years.

A new type of algorithm, the stochastic MPPT algorithm, is used to overcome this problem. This algorithm samples the function's search space and examines the full spectrum of function solutions rather than sequential analysis in the perturbation and observation process.

Nevertheless, the optimum solution cannot always be ensured, since it is in a way dependent on probability and uses a pseudo-randomness to find the global limit. Finally, it really is a reasonable way of producing the right result and, on average, improving performance. The optimum point corresponding to the MPP is always discovered if properly planned and implemented. It will of course also depend on the type of power form, as some are more or less easy to follow with this type of MPPT algorithm.

They are commonly known as heuristic or meta-heuristic algorithms that are learned on a thumb-based principle rather than on a tough, underlying theory. Although the theory of application is far behind, its findings are reasonably good.

2.3.3 Fuzzy Logic Control (FLC)

A heuristic solution can also be considered as a fluid logic control. The FLC method [15], shown in Figure 2.14, is generally three steps. The number input variables will be converted in the first stage into linguistic equivalents as input fluctuations.

Fuzzy logic, in which they have both states: true or false, is a multi-valued logic category. The logic variables therefore have values from 0 to 1, including the partial truth zone.

In the following key levels, the fugitive logic controller works:

• Fuzzification: Stage where digital values are translated into linguistic variables (the voltage and power of the field of research are usually used).

• Fuzzy rule base: Input conditions for the key variables are set by certain parameters.

• Defuzzification: The variables are translated as a multivariable function to numerical variables.

The output value of interest (MPP referral voltage) with the various parameter ranges pre-defined (irradiation, temperature, etc.) bonded to the value (power and voltage) of interest (the value of the system's power and voltage) is therefore a Blackbox function result.

Fuzzy logic control can also be called heuristic. The FLC [15] process is normally three steps as shown in Figure 2.14. The numerical variables are interpreted as fluid inputs for the first step into corresponding linguistic variables. In step two the input fuzzy sets will be translated into output fuzzy sets by comparison to the floating rule table. Finally, the output flushing sets will be transformed as the output to numerical variables.

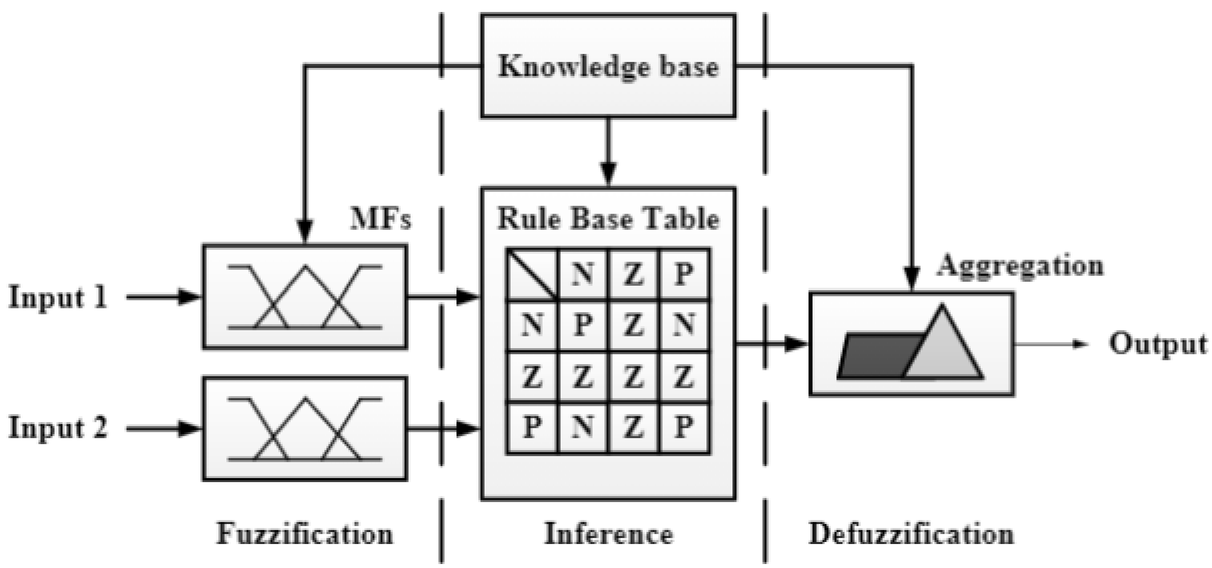

Figure 2.14: Fuzzy logical controller layout.

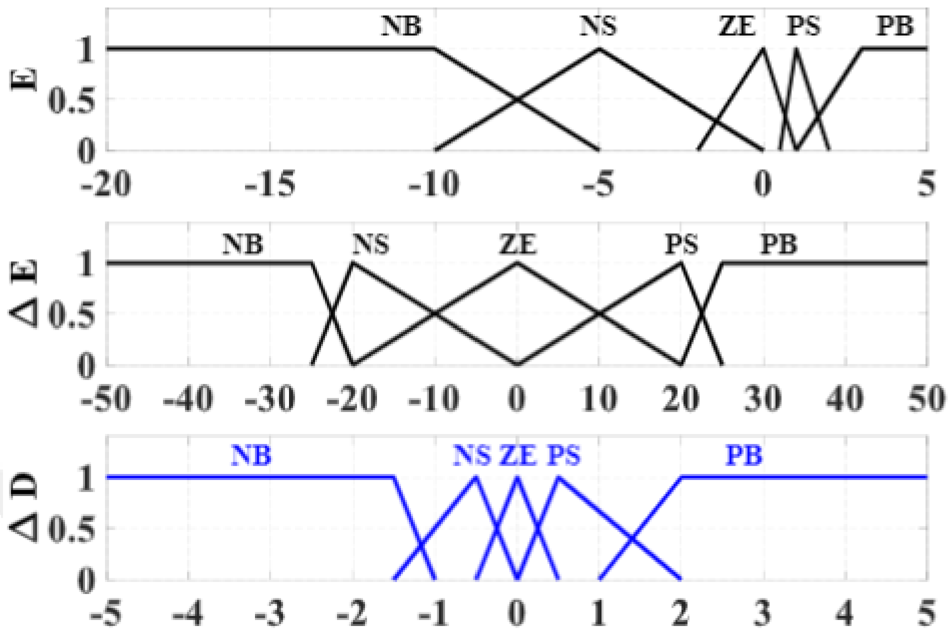

Figure 2.15: Membership functions of five fuzzy levels.

Figure 2.16: Five fluffy-level rule base table.

E \ ΔE	NB	NS	ZE	PS	PB
NB	PB	PB	PS	PB	PB
NS	PB	PS	PS	PS	PB
ZE	NS	NS	ZE	PS	PS
PS	NB	NS	NS	NS	NB
PB	NB	NB	NS	NB	NB

In general, the FLC approach has improved its efficiency in various atmospheric conditions compared to other heurist methods [56–58]. The efficiency of the FLC is, however, heavily dependent on the system's design expertise. For example, there is a high number of fluffy rules, which makes FLC design and implementation more difficult.;

2.3.4 Hybrid Method

2.3.4.1 MPP-locus Method

M. D and Sokolov. In [44], the traditional MPP-Locus approach was offered by Shmilovitz. Figure 2.17 illustrates the central theory of this approach.

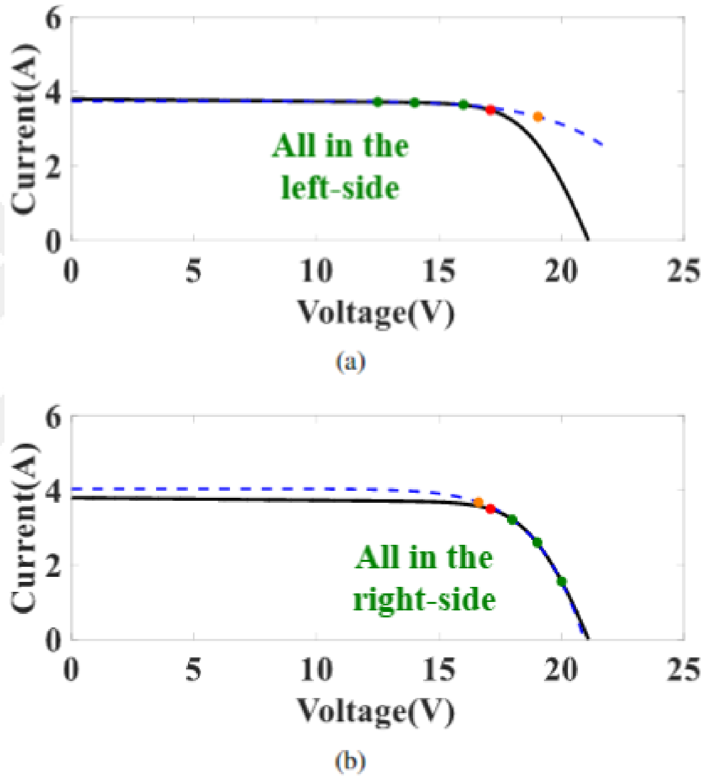

Figure 2.17: Poor position selection for three pairs of voltage and electricity: (a) all dots on the left side; (b) all dots on the right side.

The position of the MPPs in the various solar irradiances is almost emulated straight lines as shown in Figure 2.17[65]. This approach is based on the fact that the operating point is always to hold almost on the direct line, in order to minimize tracking time. If, for example, the weather situation is altered, from point 1 to point 2 the operating point varies. The operating point is then moved directly to point 2 with the MPP Locus procedure. The advantages of this method are its excellent dynamical efficiency, particularly in cases of unexpected changes in solar irradiance.

The P&O or INC form is often used to find the MPP site accurately. However, under low solar radiation or different temperature conditions, this system has poor monitoring efficiency [46]

2.3.4.2 Beta Method

Beta is a special method of MPPT. Contrary to the previously stated MPPT methods, the principle of Beta is shown in [47] and the intermediate variable β is given as an intermediate variable, instead of power or voltage:

$$\beta = In\left(\frac{I_{pv}}{V_{pv}}\right) - c \times V_{pv} \qquad (2.16)$$

Where c=q/(NsηkT) is the diode constant.

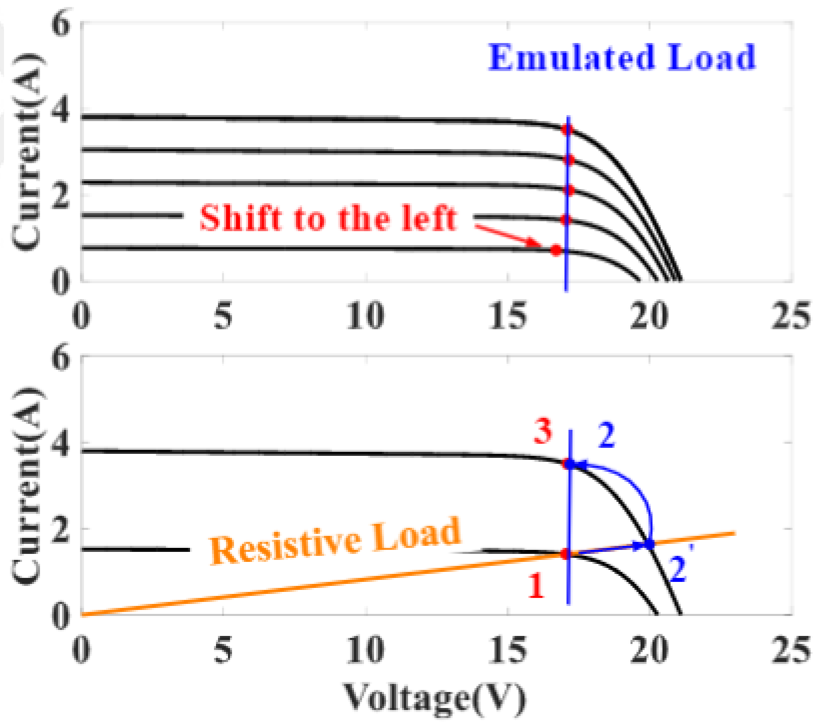

Figure 2.18: Basic principle of the MPP-Locus method

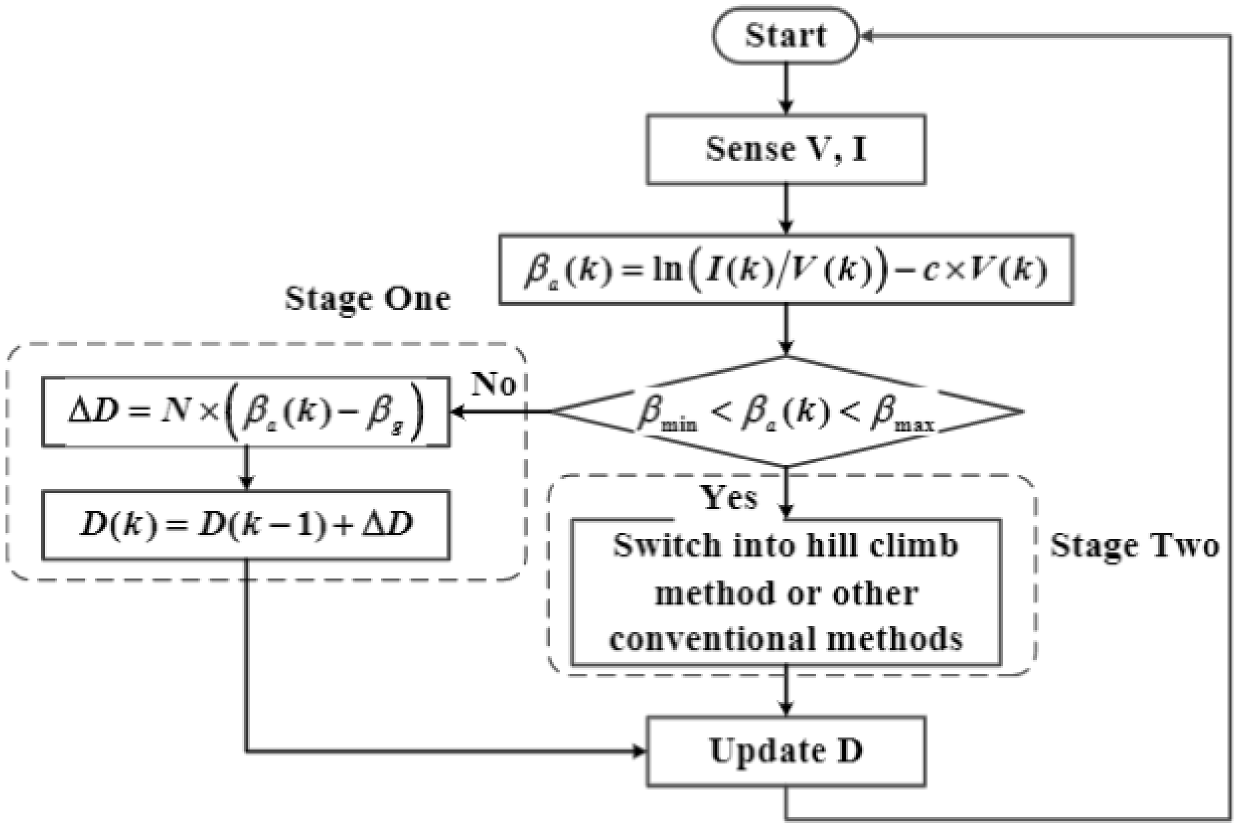

Figure 2.19: Flowchart of the Beta method.

2.3.4.3 Combined MPPT algorithms

The system has extra robustness against partial shade from stochastic algorithms, but at the same time it makes it in various scenarios less effective. A diverse way of dealing with this search control mechanism is to use the two previously described different kinds of algorithms, to avoid an approx. local limit, using a stochastic one, and then to hold this mechanism within a small, closer area with a global maximum using a deterrent approach. On the opposite, the deterministic approach is maintained in order to define a new global limit that has varied in negligible quantities, ensuring an improved performance on the device, since the deterministic method is usually quicker and more reliable. This is a method that combines a main routine code with the traditional algorithm with the subroutine code which triggers a new power shape when looking for the area containing the MPP.

2.4 SUMMARIZATION OF THE REVIEWED AFOREMENTIONED MPPT METHODS

The above MPPT methods analyzed have been summarized in Figure 2.20. As discussed earlier in the previous section, these MPPT methods are classified into three categories. The MPPT methods have 8 common functions which are summarized and outlined at the bottom of Figure 2.20. These eight MPPT-related characteristics apply to the 3 different colors, neutral and positive. -- of these MPPT strategies must clearly be evaluated in Figure 2.20. Most MPPT methods can monitor the true MPP with the exception of linear approximation. The above MPPT methods analyzed have been summarized in Figure 2.20. As discussed earlier in the previous section, these MPPT methods are classified into three categories. The MPPT methods have 8 common functions which are summarized and outlined at the bottom of Figure 2.20. These eight MPPT-related characteristics apply to the 3 different. -- of these MPPT strategies must clearly be evaluated in Figure 2.20. Most MPPT methods can monitor the true MPP with the exception of linear approximation.

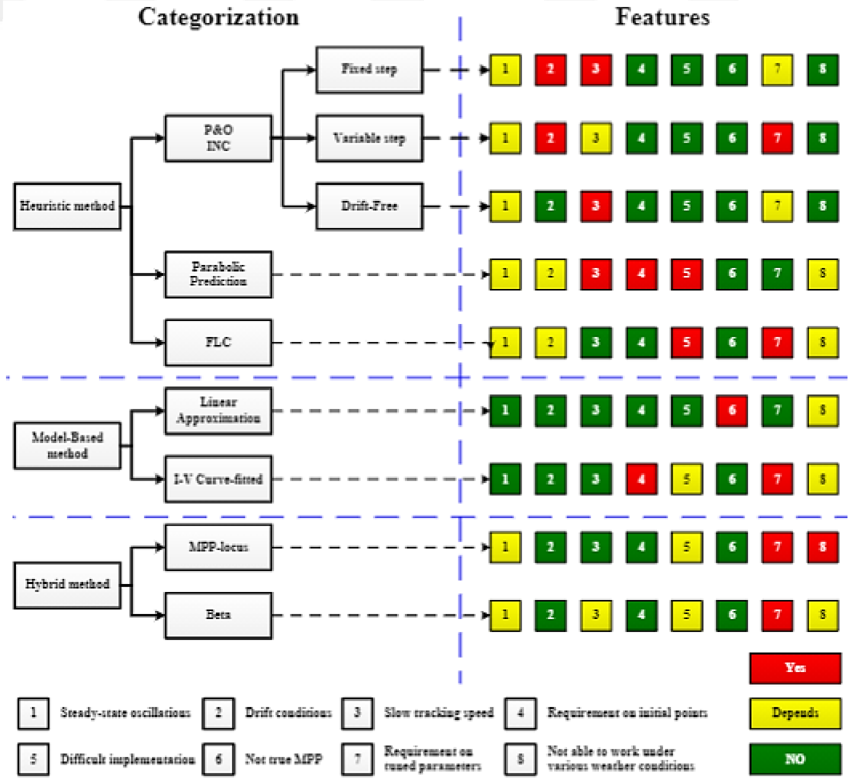

Figure 2.20: Description of the MPPT methods discussed above.

2.5 CONCLUSION

The suitability of technologies for full power extraction in partial photovoltaic shading conditions was investigated. This research emphasizes the follow-up of global MPPs and hence the best duty value for extractive power under partial shading. Several optimization techniques have been analyzed to study the output power and tracking efficiency of partially shaded PV system. Various PV power processing architectures such as central, string and DPP have been analyzed to study the output power, convergence speed and efficiency of PV array under partial shading condition. It is proved that the DPP architecture with GWO algorithm is the best suited one for PSC.

This chapter offers a comprehensive description of MPPT solar radiation norm and uniform algorithms. While comprehensive literature on MPPT is available for uniform solar radiation, very few algorithms are available in MPPTs for uniform solar radiation. conventional P&O, Gradual Lead etc. MPPT algorithms. are not optimal when multiple peaks are present around a PV curve to extract maximum power from PSCs. Consequently, global MPPT optimisation techniques to manage the various MPPs for stochastically varying solar radiation should be established.

3. METHODOLOGY

3.1 INTRODUCTION

The output power and efficiency of the PV panel not only depends on the irradiance and temperature value and also depends on architecture. Hence, various architectures such as central, string and Differential Power Processing (DPP) are discussed in many literatures (Ahmed A. Elserougi et al. 2015 [48]; Kim et al. 2015 [49]; Pradeep Shenory et al. 2013 [50]; Young-Tak Kim et al. 2017) For a partial shading system. PV system. The DPP design using a boost converter is among those most promising for partial shading conditions. Therefore, in this research work DPP architecture along with Grey Wolf Optimization (GWO) has been analyzed Maximum monitoring power point for partial shading.

3.2 METHODOLOGY

PV system with DPP architecture employing Grey Wolf Optimization (GWO) technique under partial shading condition is presented in this chapter. The DPP architecture processes only the difference power between panels so that panel currents are uniform under partial shaded condition, which enhances the conversion efficiency. The block diagram of PV system considered for analysis in this chapter is the same as the earlier system in chapter 2, except the architecture and MPPT algorithm as shown in Figure 3.1. In this research work, the last two chapters deal with power extraction from PV panel under PSC using different optimization algorithms such as PSO, GSA, PSOGSA, RDPSO and FPA. In this chapter, along with power extraction various architectures are also discussed to improve the efficiency.

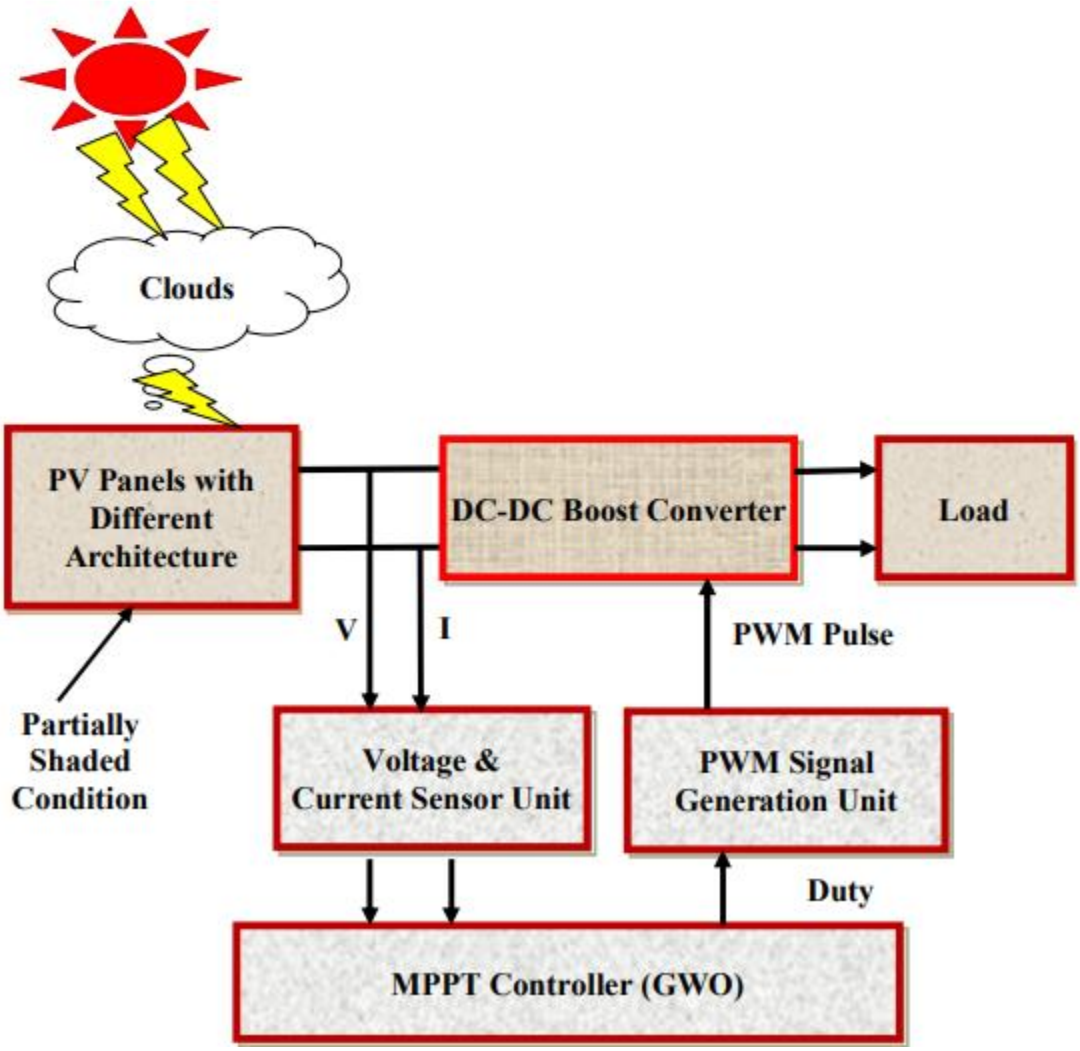

Figure 3.1: Proposed PV system with GWO Technique

3.3 PV ARCHITECTURE

One of the factors to improve the tracking efficiency of the PV system under PSC is how the PV panels are connected to the load. Different architectures for PV system have been developed to enhance the power processing capability and in turn the power conversion efficiency. Description of different PV system architectures are presented in the following sections.

3.3.1 Central Architecture

In central architecture, a single boost converter processes the total power of the PV panel. All the PV panels are connected in series or in series parallel combination and then connected to the boost converter. In this research work, the series combination of PV panels with a single boost converter has been selected as shown in Figure 3.2.

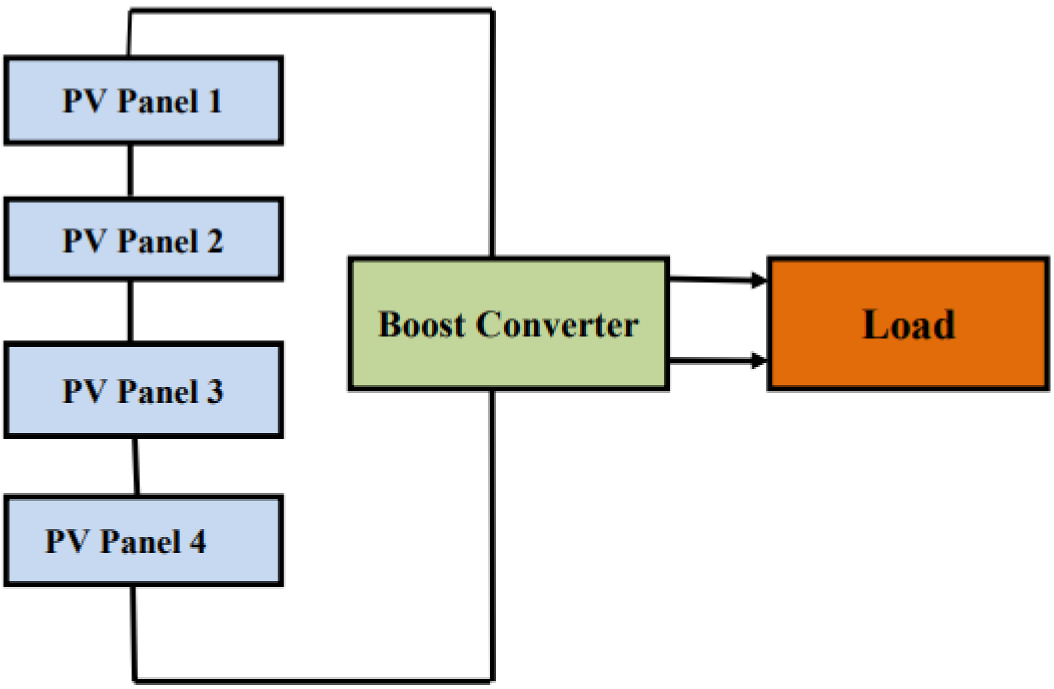

Figure 3.2: Central Architecture

Central architecture connects four PV panels with the central boost converter in series as it extracts the full power from the overall panels of photovoltaic systems that are lower than the amount of the maximum potential of each table panel because of partial shade losses (Ahmed A. Elserougi et al. 2015) [51]. This architecture is efficient when the operating conditions are uniform but have a reduced power output due to shading of PV panels (Pradeep S. Shenoy et al. 2012) [50].

3.3.2 String Architecture

In this architecture, PV panels are connected to form strings and each PV string has two PV panels connected in series for each series, the Boost Converter performs MPPT Control as shown in Figure 3.3. The strings are connected parallel to the load. The string voltage and current from each string is usually sensed to perform MPPT control.

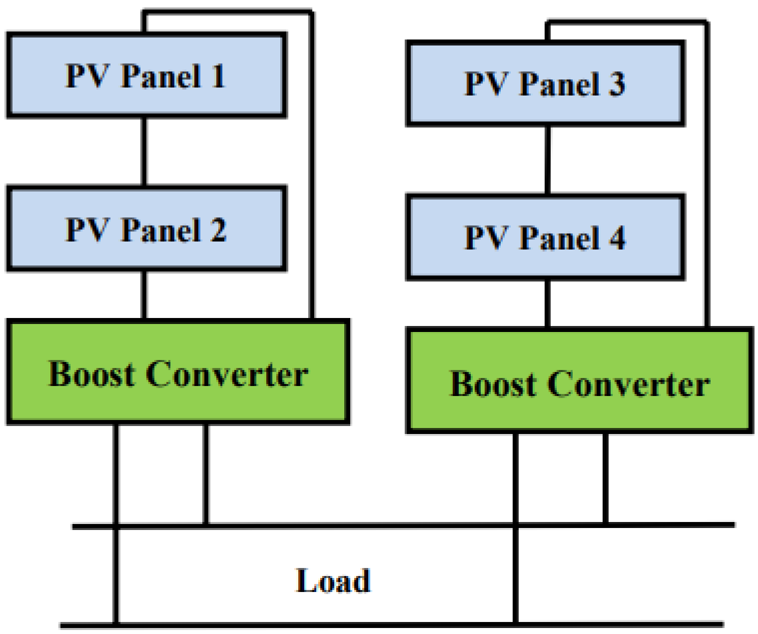

Figure 3.3: String Architecture

The benefit of a string architecture is that MPPT is done on string level by string converters. Therefore, under various situations the performance of the MPPT is higher than the central architecture. But under the same conditions, the string architecture approach still has substantial power losses. The explanation is typically that a bypass diode is mounted parallel to each panel when the PV panels are attached to a string as shown in figure 3.4.

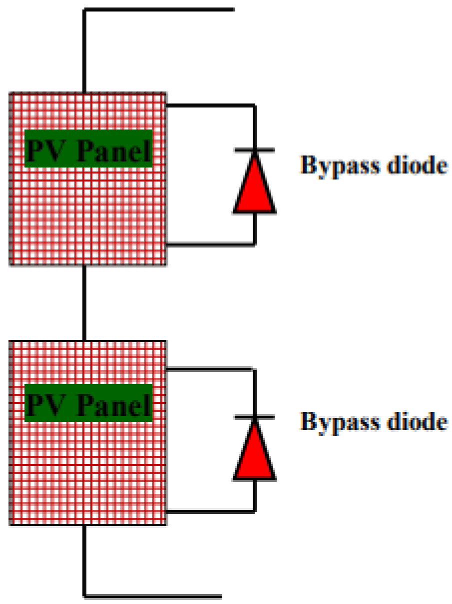

Figure 3.4: PV panel with bypass diode

This is so shaded that if a PV panel is shaded, the current level of the PV-panel is stored within the same chain. Thus, the power of the bypassed panels is lost when PV panels work under unequal conditions. When neither panel uses circumvented diodes, a shaded string panel contributes to a major power loss as the shaded panel restrains the string current because of its series relationship.

3.3.3 Differential Power Processing Architecture

In differential power processing architecture, each panel has an individual converter and is connected as shown in Figure 3.5 (Kyoung-Tak Kim et al. 2017) [52] in order to process only the difference power between the two consecutive PV panels, under partial shading condition.

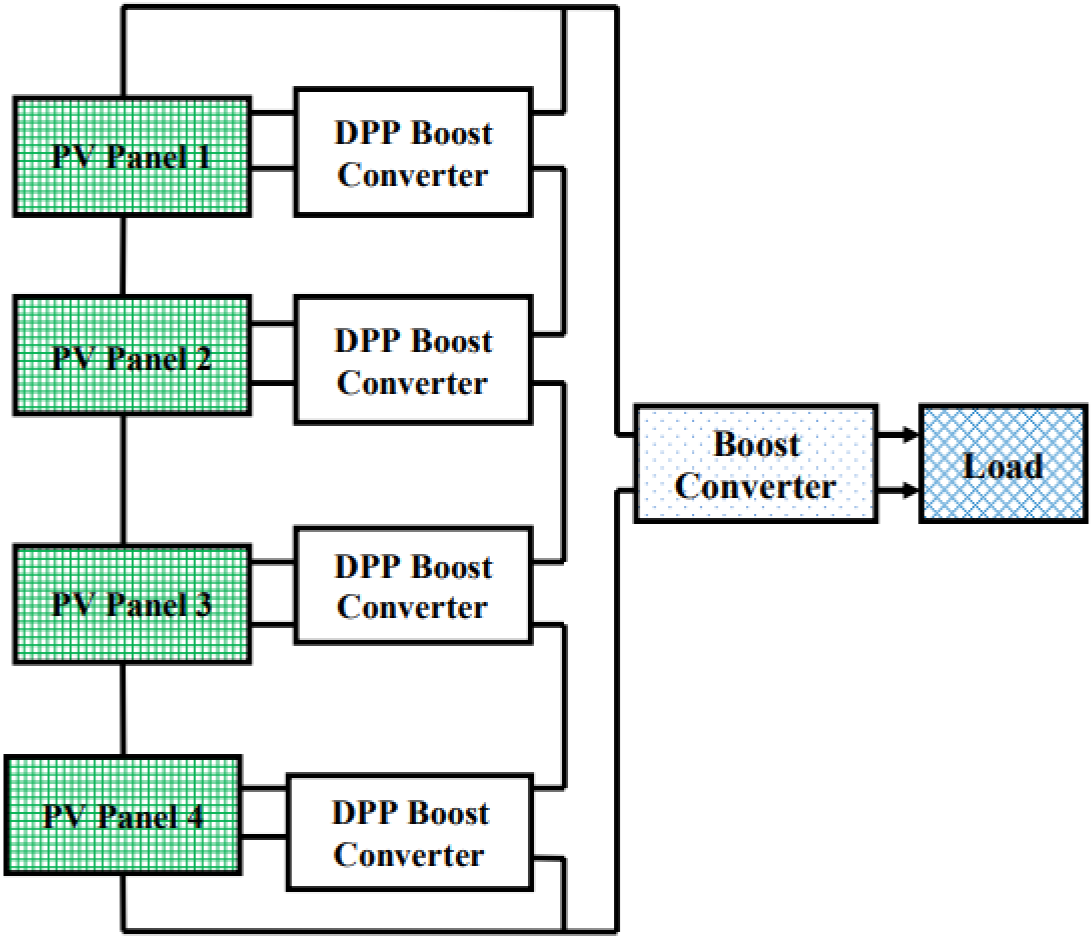

Figure 3.5: DPP Architecture with boost converter

When PV cells are connected in series there exists an internal and external mismatch problem which reduces the output power. This drawback is overcome by Differential Power Processing (DPP). Each injects an additional current that matches the generated PV current with the general string current.

The majority of the current therefore flows directly into the chain, without the DC / DC converters being processed. This is why differential architectures provide great advantages: only a small fraction of the total power is processed, and the device performance can be very high because conversion errors only affect the processed power. No power is stored, and machine efficiency is 100 percent, if all substrate matches the same currents. The power that the DPP converter processes is calculated,

$$P_{conv.DPP} = \sum\left|V_{pv.ind} - V_{dc}\right| I_{pv.ind} \quad (3.1)$$

Where Vpv,ind is individual PV panel voltage, Vdc is the dc bus voltage of the PV system, and Ipv, ind is individual PV panel current.

Thus, this research ultimately compares central, string and differential power processing architecture with GWO technique and the results are compared with PSO and RDPSO algorithms. The research outcome is the selection of the best architecture that can be implemented in practice so that maximum power can be extracted from PV panel under PSC. The following section offers a brief discussion on the gray wolf optimization technology to identify the optimal duty value to extract MP from PV array under PSC.

3.4 GREY WOLF OPTIMIZATION (GWO)

Mirjalili et al. (2014) [26] proposed a GWO algorithm that resembles the leadership qualities and hunting behaviour of grey wolves in nature. Grey wolves prefer to live in a group. The average wolf group size is 5-12. The leadership hierarchy consists of four types of grey wolves called alpha (Ị), beta (ü), delta (ị), and omega (Ȧ). Among this alpha is the leader and it may be a male or a female.

It is the alpha wolf who determines hunting, how to sleep, when to wake up, etc. The actions of the alpha are the laws that the wolf community must obey. Alpha wolf may not be the strongest wolf in the group but must be able to influence the group. The next level of hierarchy in the grey wolves is beta and it may be either a male or female.

In case alpha wolf loses its life or is aged, then the beta wolf becomes the leader. Normally, a beta wolf is an assistant wolf to alpha, that helps the alpha in decision-making, or any other activities and it is the best coordinator to the alpha wolf. The beta wolf commands and controls the other lower-level wolves but it should respect the alpha. It acts as an advisor to the alpha and discipliner for the other wolves in the group.

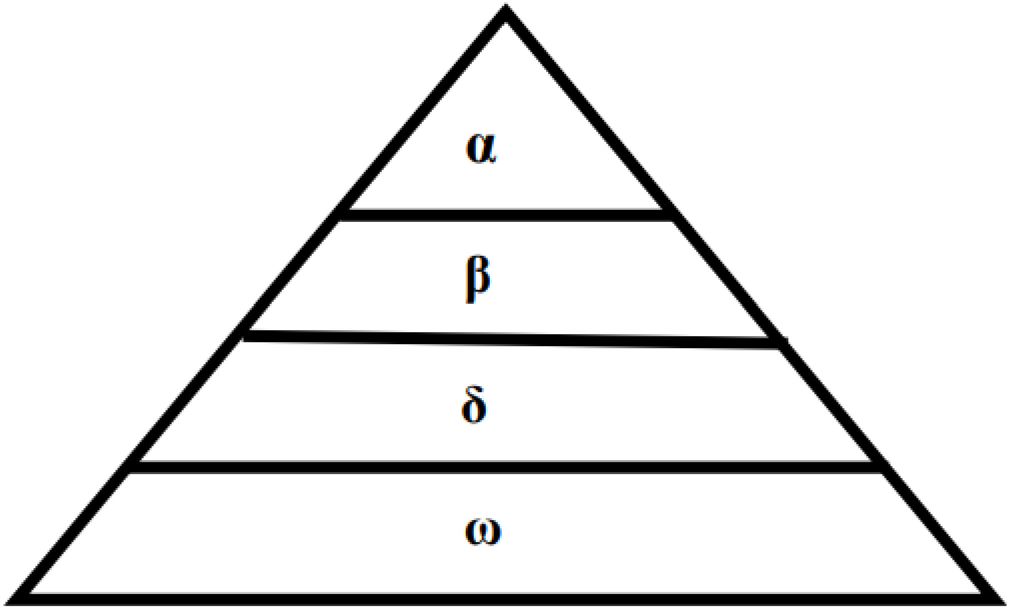

Figure 3.6: Hierarchy of grey wolf

The beta wolf conveys the alpha's messages to other wolves in the group and collects the feedback from the group and conveys the feedback to alpha. The least rated grey wolves are called omega and they are the first ones to attack the prey and eat. If a wolf is not an alpha, beta or omega then the remaining wolves are called delta and they perform duties like guarding, care taking of elders, etc.

The hierarchy of grey wolf is shown in Figure 3.6. The main steps of grey wolf hunting are shown in Figure 3.7.

- Follow, pursue and approach the prey.
- pursues the prey, surround them and annoy them before they stop moving.
- Attacking the prey

Figure 3.7: Gray wolves hunting conduct: (a) chasing, harassing, and circulating (e) stationary condition in pursuit, approaching and tracking prey (B-D) (Seyedali Mirjalili)

3.4.1 Mathematical Model of GWO Algorithm

The mathematical model of the social hierarchy, tracking, encircling and attacking prey of GWO algorithm is outlined in this section.

(a) Social hierarchy

In order to model the social hierarchy of wolves in GWO technique, Assume the fittest solution as the alpha (Į). And it is followed by the second and third best solutions, namely, beta (ȕ) and delta (į), respectively. The rest of the candidate solutions are assumed to be omega (Ȧ). The hunting mechanism is guided by alpha, beta and delta. The omega wolves follow these three wolves.

(b) Search for prey (exploration) and Encircling prey

Gray wolfs surround a beast during hunting, and the surrounding behavior is influenced by the following.

The distance D of a wolf from the prey can be estimated by Equation (3.2).

$$\vec{D} = \left|\vec{C} \times \vec{X}_P(n) - \vec{X}(n)\right| \tag{3.2}$$

$$\vec{X}(n+1) = \vec{X}_P(n) - \vec{A} \times \vec{D}$$

Where the position of n is indicated, a and c vectors are coefficient, Xp is called the vector position of the prey, and X is a vector of the gray wolf. For evaluating the value, A and C, equations (3.3) and (4.4) are used.

$$\vec{A} = 2\vec{a}.\vec{r}_1 - \vec{a} \tag{3.3}$$

$$\vec{C} = 2\vec{r}_2 \tag{3.4}$$

The 'a' linear decrease from 2 to 0 and r1 are random vectors with a value of 0 to 1. By changing the value of A and C vectors, the best solution can be obtained by using the current location. A wolf will enter a location between the random vector r1 and r2 points. A grey wolf can then randomly upgrade its position using equations (3.1) and (3.2) Equations.

(c) Hunting

In hunting mechanism, the grey wolves encircles the prey and then moves towards the prey. When a desired distance is reached the wolf starts attacking the prey. The hunt is usually guided by the leaders' wolf called alpha followed by sub leader beta and delta occasionally participates in the hunting mechanism.

The updating of the position of a wolf in a 2D search space based on the position of alpha, beta, and delta is shown in Figure 4.8. In a circle identified by alpha, beta and delta positions in the search space the final position will be located in a random spot. Second, the location of the alpha, beta and delta is updated, and all the wolves are updated randomly around the presa.

In order to mathematically model the hunting behaviour of grey wolves, the distance of the wolves from the prey are updated using Equations (3.1) and (3.2). First three best solutions obtained at any iteration are considered as alpha, beta and delta.

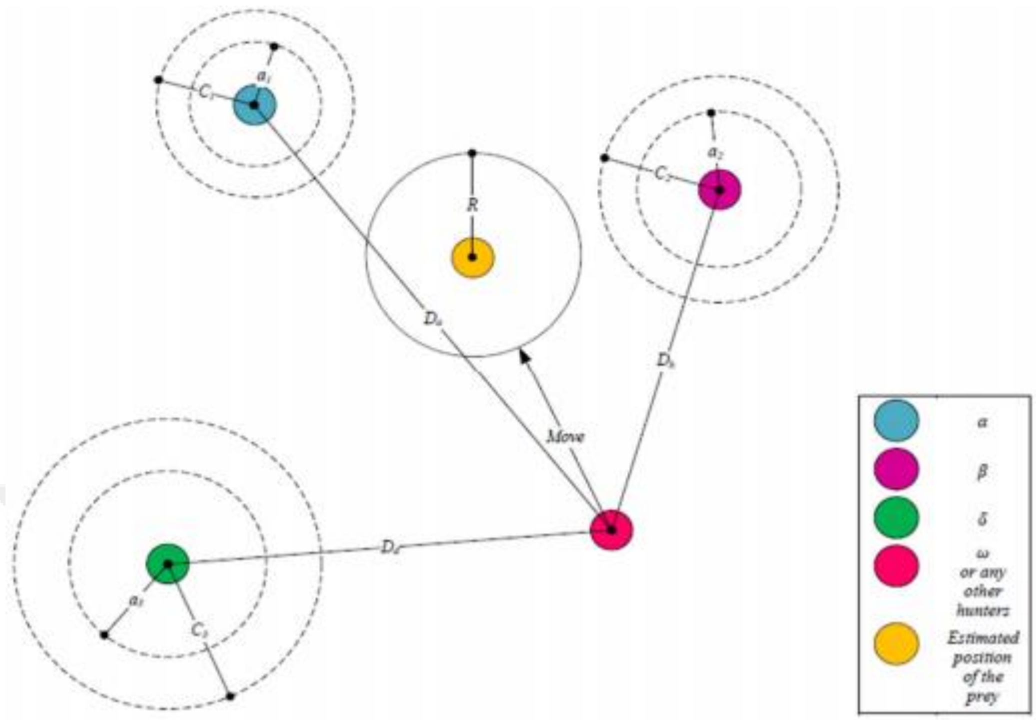

Figure 3.8: Position updating in GWO (Seyedali Mirjalili) [26]

The average of these three solutions is used to update the distance in the next iteration. The equations used to update the position of alpha, beta and delta are listed ahead.

$$\overrightarrow{D_a} = \left|\overrightarrow{C_1} \times \overrightarrow{X_a} - \vec{X}\right| \tag{3.5}$$

$$\overrightarrow{D_\beta} = \left|\overrightarrow{C_2} \times \overrightarrow{X_\beta} - \vec{X}\right| \tag{3.6}$$

$$\overrightarrow{D_\delta} = \left|\overrightarrow{C_3} \times \overrightarrow{X_\delta} - \vec{X}\right| \tag{3.7}$$

$$\overrightarrow{X_1} = \left|\overrightarrow{X_\alpha} - \overrightarrow{A_1} - \overrightarrow{D_\alpha}\right| \tag{3.8}$$

$$\overrightarrow{X_2} = \left|\overrightarrow{X_\beta} - \overrightarrow{A_2} - \overrightarrow{D_\beta}\right| \tag{3.9}$$

$$\overrightarrow{X_3} = \left|\overrightarrow{X_\delta} - \overrightarrow{A_3} - \overrightarrow{D_\delta}\right| \tag{3.10}$$

$$\vec{X}(n+1) = \left({\overrightarrow{X_1} + \overrightarrow{X_2} + \overrightarrow{X_3}} \Big/ {3} \right) \tag{3.11}$$

(d) Attacking prey (exploitation)

When it stops moving the gray wolves complete the chase by attacking the prey. 'A' vector may be a random value between [-a, a] where, during iterations, a decreased from 2 to 0. The next position of a search agent between the present position and the position of the bear is when random values are set in [-1, 1]. If the Figure 3.9 (b) indicates the.

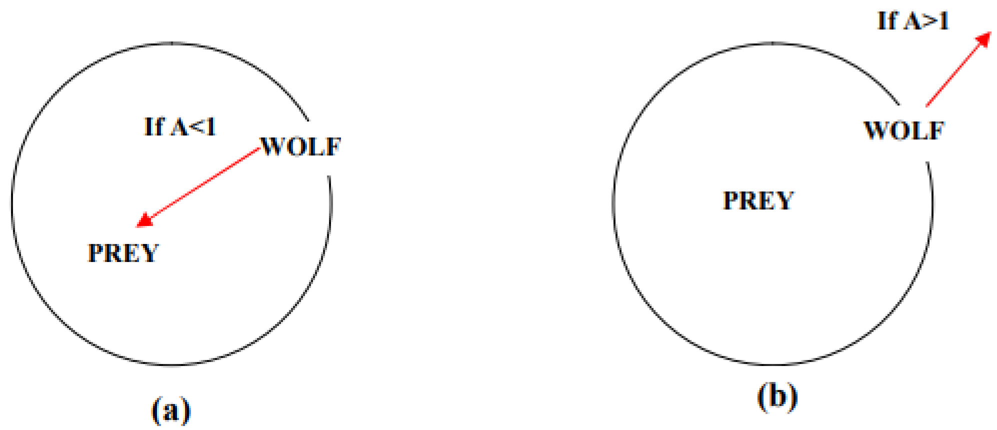

Figure 3.9: Attacking prey versus searching for prey

(e) Fitting GWO for PSC PV MPPT tracking

In general, GWO algorithm is applied to optimize the positions of a group of wolves or particles (N) moving towards a prey or objective. Therefore, the algorithm starts with the initial actual position (X) of a wolf and an assumed best position (G) of wolf.

The optimisation process involves k iterations to determine the best position of the wolf. Hence, in an iteration called nth iteration, there will be nth iteration value for position on N wolf, is namely, X1,n, X2.n,.....Xi,n,....,XN,n. The algorithm has to determine n+1th iteration value of the position, which is determined using equations (3.1) and (3.2).

In this research work, GWO algorithm is applied to optimize the duty of number of wolves (N) moving towards an objective which is maximum power. Therefore, the algorithm starts with initial duty (X) of a wolf and an assumed best position (G) of wolf. In iteration the duty is updated, and the search process ends after k iterations.

3.4.2 GWO Algorithm Steps

The measures below are used for controlling PWM 's best task to obtain full PV PSC Capacity.

Step 1: Select an initial Wolves Group (N) and iteration number (k).

Step 2: Can objective or variable fitness maximum power (PMAX).

Step 3: The PWM duty of the Wolves is the variable to achieve objective.

Step 4: For PWM duty pick the upper and lower limits.

Step 5: Generate PWM duty for each Wolf.

Step 6: Generate initial fitness power for each wolf, sort them in descending order, set first highest three as alpha, beta and delta. Set the power corresponding to alpha as Pmax and duty as Gbest.

Step 6a: Start nth iteration by running simulation with PWM duty of each Wolf and get power, Pn, I for nth iteration for all the Wolf.

Step 7: Sort the power Pn, i in descending order.

Step 8: Update the Alpha, Beta and Delta using the first three highest of power.

Step 9: If power corresponding to alpha is greater than Pmax, then set this power as Pmax and corresponding duty as Gbest of nth iteration.

Step 10: For the next iteration, evaluate the variation between the actual PWM duty and the corresponding PWM duty for Alpha, Beta and Delta. Take the difference average and use the average to create the next iteration's PWM duty.

Step 11: Repeat next iteration with new PWM duty.

Step 12: In iterations the PWM duty (Gbest) is updated.

Step 13: Iterations are stopped after k iterations. The value of Gbest at the end of k iterations is the desired duty for MPPT. Figure 3.10 shows the flowchart of GWO algorithm.

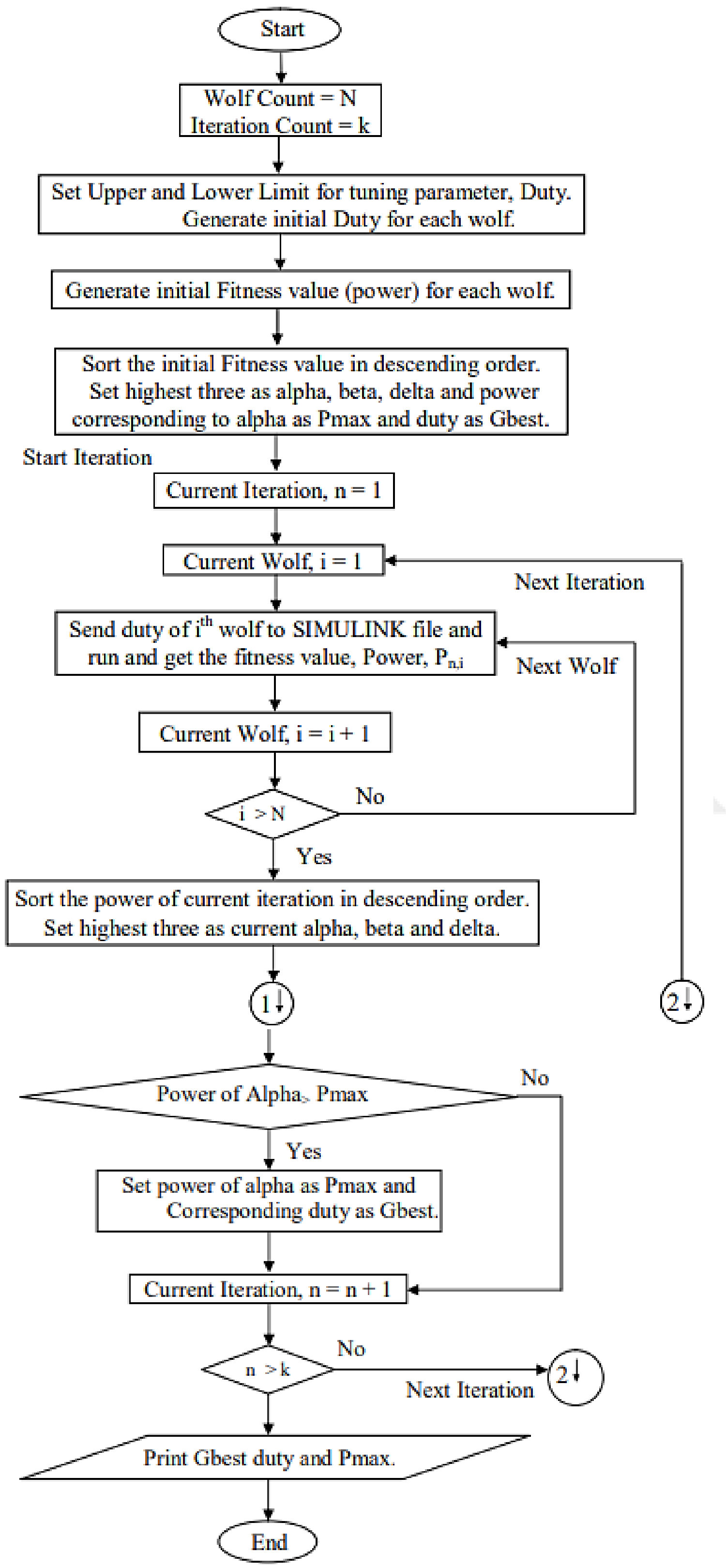

Figure 3.10: Flow chart of GWO algorithm

3.5 SIMULATION RESULTS AND DISCUSSION

The performance of the PV system is analyzed under partial shading condition. Four PV panels are assumed and the irradiance levels for four panels are 1000W/m2, 800W/m2, 600W/m2, 400W/m2. Using this irradiance levels PV system is simulated using the specifications given in Table 2.2. The parameters assumed for different algorithms are tabulated in Table 3.1.

Table 3.1: Parameters for various optimization algorithms

PSO	RDPSO	GWO
Number of iterations=10	Number of iterations=10	Number of iterations=10
Number of Swarm=10	Number of Particle=10	Number of Wolf=10
Inertia weight (W)=1	alpha_max=0.9 alpha_min=0.3 beta=1.5 Acceleration Coefficient(C_1=0.2) C_2=C_1	a_{max} = 2 a_{min} = 0

3.5.1 Central Architecture

The Simulink model of central architecture is shown in Figure 3.11. It consists of four PV arrays connected in a series and this combination is connected to the boost converter and load. Irradiance values for four PV panels are 1000W/m2, 800W/m2, 600W/m2, 400W/m2 and the temperature is 25C and it is constant for all the PV arrays.

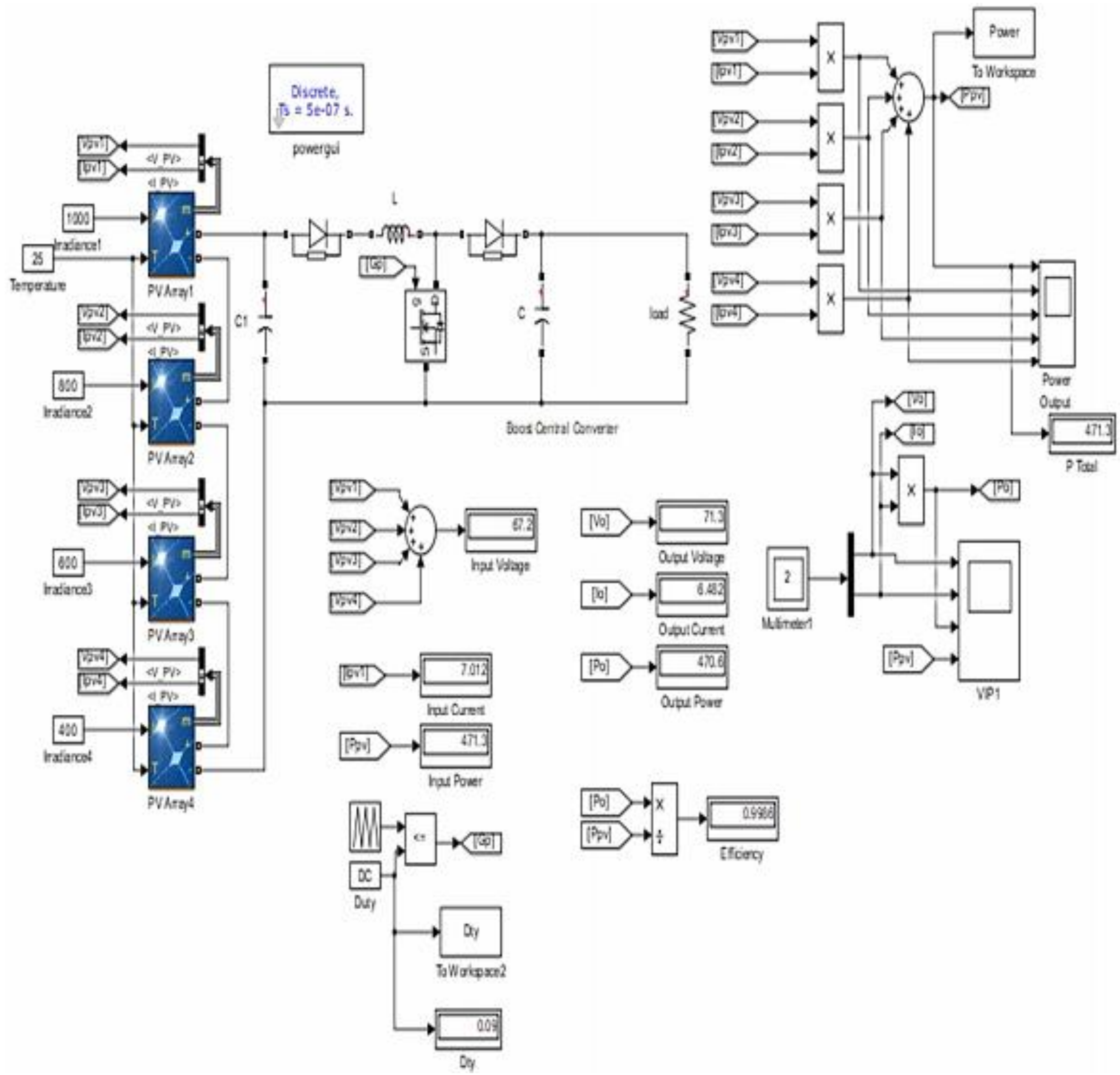

Figure 3.11: Simulink model of central architecture

Under uniform irradiance condition power extracted from the PV array is more (960W) when compared to non-uniform irradiance condition. This architecture is not suitable for non-uniform irradiance values because the maximum overall characteristic of the PV array that can be less than the amount of the maximum available power of any panel can be extracted in the PV array.

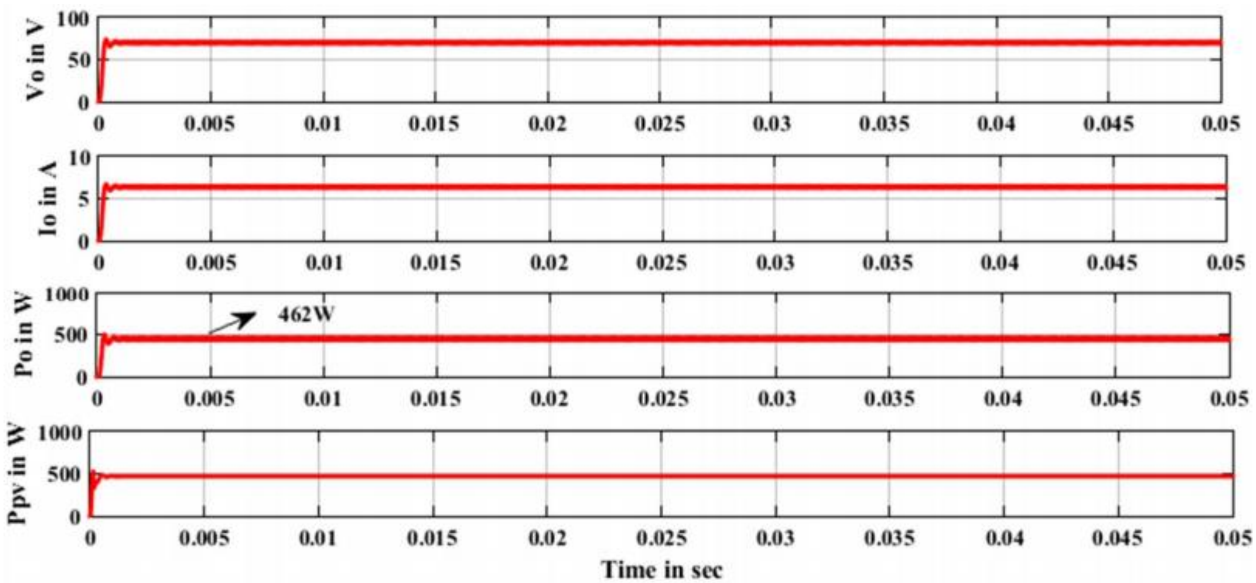

Figure 3.12: Output voltage, current, power and panel power of central architecture using PSO

It is observed from the simulation result shown in Figure 3.12 that 98.04% of power is tracked from its maximum value (471.2W). Power reaches its steady state value at t=0.021s. The output power obtained using the PSO algorithm under PSC is 462W.

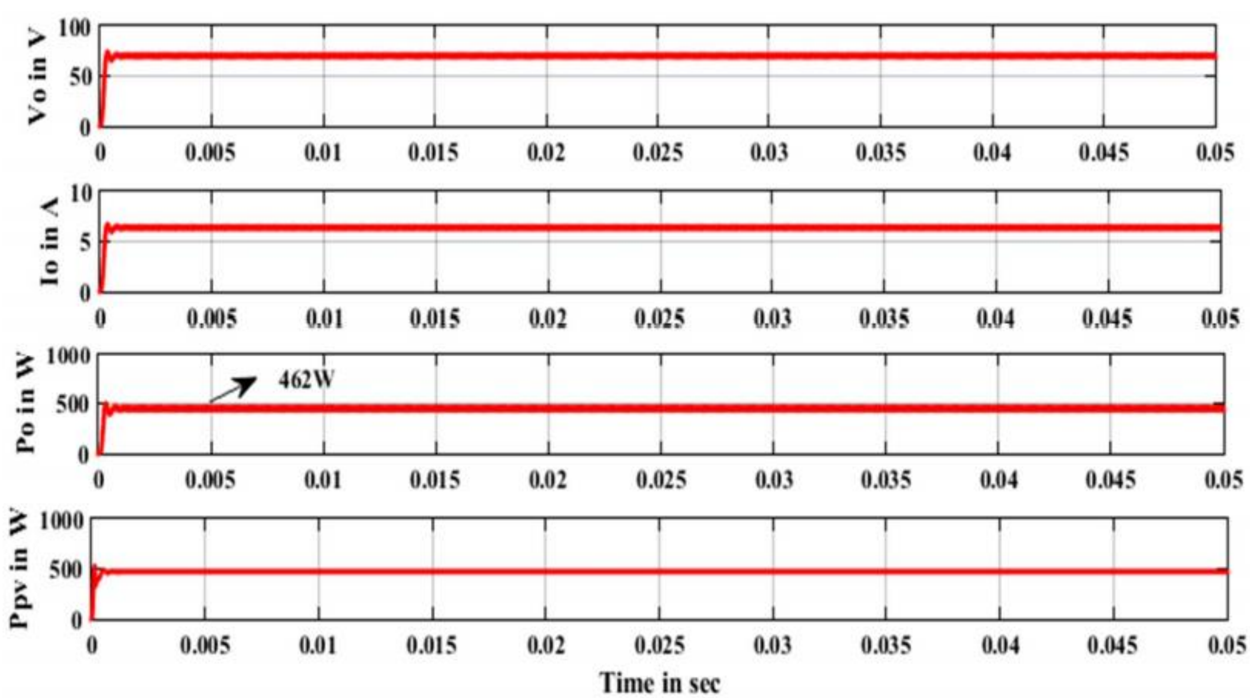

Figure 3.13: Output voltage, current, power and panel power of central architecture using RDPSO

The simulation of output voltage, current and power obtained from PV arrays using RDPSO algorithm is presented in Figure 3.13. It is noticed from the results that output power reaches the steady state value very slow, but more oscillations are present compared to PSO algorithm.

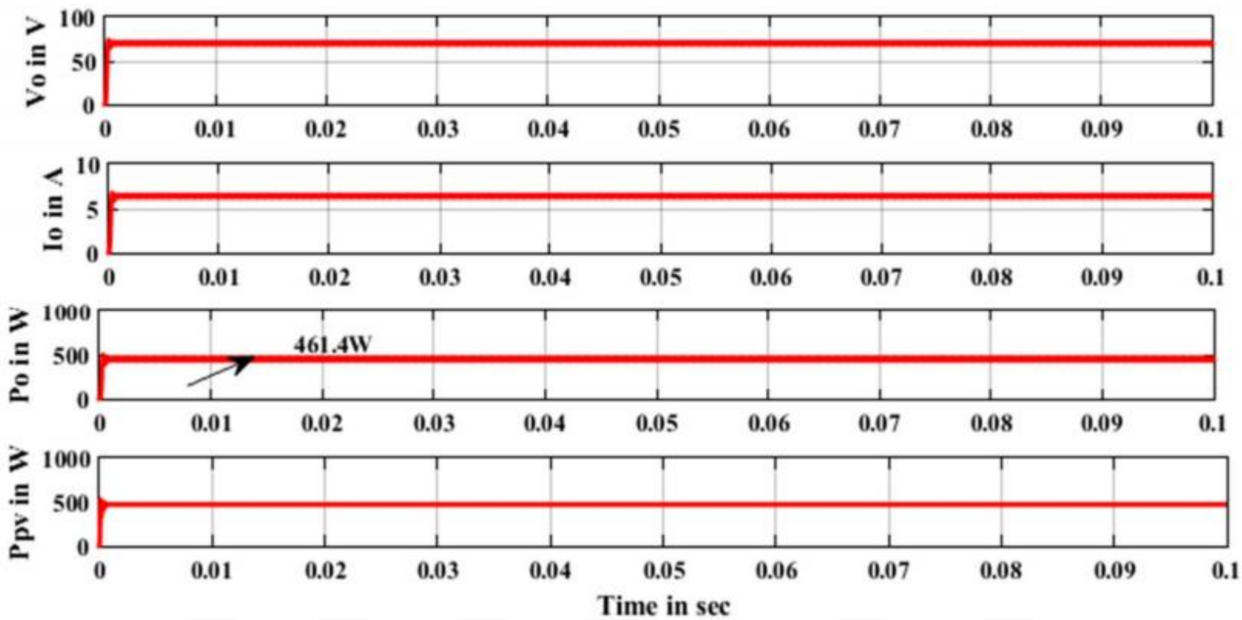

Figure 3.14: Output voltage, current, power and panel power of central architecture using GWO

P-V characteristics indicate a maximum power of 471.2W. Power extracted by using the gray wolf technique from PV panels is 471.2 W. In contrast with PSO and RDPSO, power extracted using GWO is higher as shown in Figure 3.14 and it reaches a GPP very fast, and it reaches the steady state value at 0.019s. The simulation results are tabulated in Table 3.2 and also conversion and tracking efficiency are calculated using the below formulas.

Conversion efficiency = (Output Power / Input Power) ×100 (3.12)

$$= (P_0/P_{pv}) \times 100$$

Tracking efficiency = (Power obtained from the PV panels/ Maximum power obtained from the P-V curve) × 100 (3.13)

$$= (P_{pv}/P_{max}) \times 100$$

Table 3.2: Performance of central architecture using various algorithms

P_{max} (W)	Algorithm	Architecture	V_{pv} (V)	I_{pv} (A)	P_{pv} (w)	V (V)	I_O (A)	P_o (w)	Converter Efficiency (%)	Tracking Efficiency (%)
471.2	PSO	Central	66.23	7.101	470.3	70.97	6.451	462.0	98.24	99.80
	RDPSO		66.23	7.101	470.4	70.97	6.451	462.0	98.21	99.83
	GWO		67.19	7.014	471.2	70.92	6.447	461.4	97.91	100

It is observed from the Table 3.2, that the power extraction in central architecture under partial shading using GWO is 471.2W. Power extracted is more in GWO technique compared to PSO and RDPSO algorithms.

3.5.2 String Architecture

It offers MPPT on a string level with all strings separate each other, thereby eliminating partial shading losses. Two strings in each string are linking two PV panels in series with MPPT, as shown in Figure 3.15 (a), and this architecture includes two strings. The string architecture's power-voltage properties are shown in Figure 3.16(b), and Figure 3.17(c) is shown for convergence.

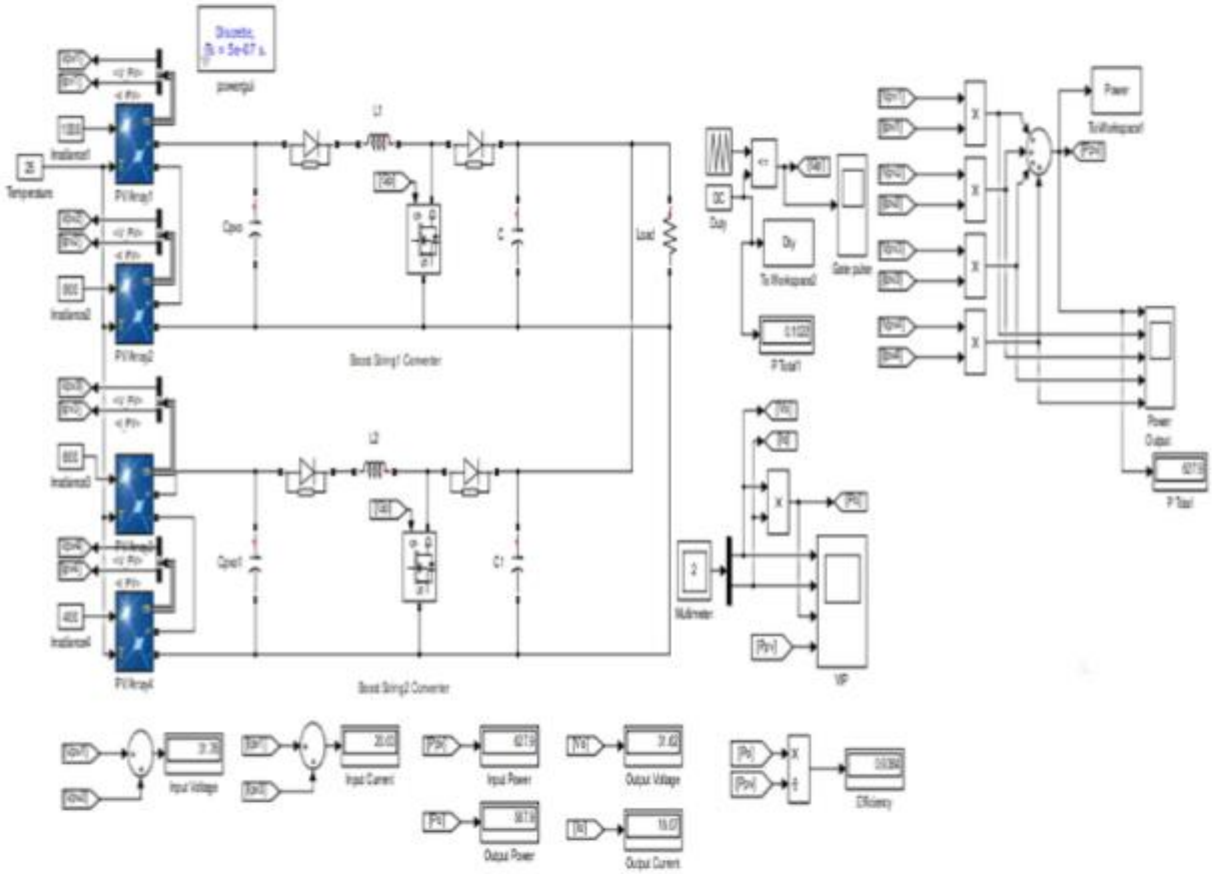

Figure 3.15: (a) Simulink model of string architecture with GWO technique

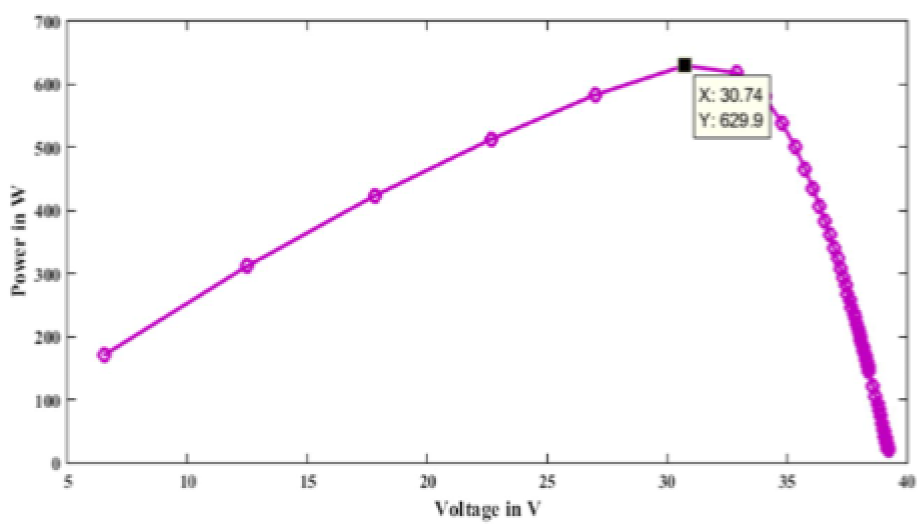

Figure 3.16: (b) Power-Voltage characteristics of string architecture

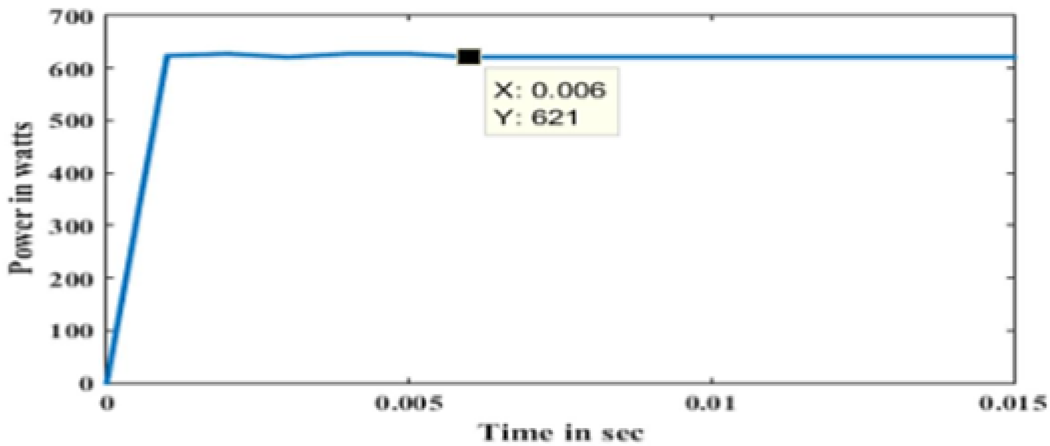

Figure 3.17: (c) Power Vs Time for string architecture

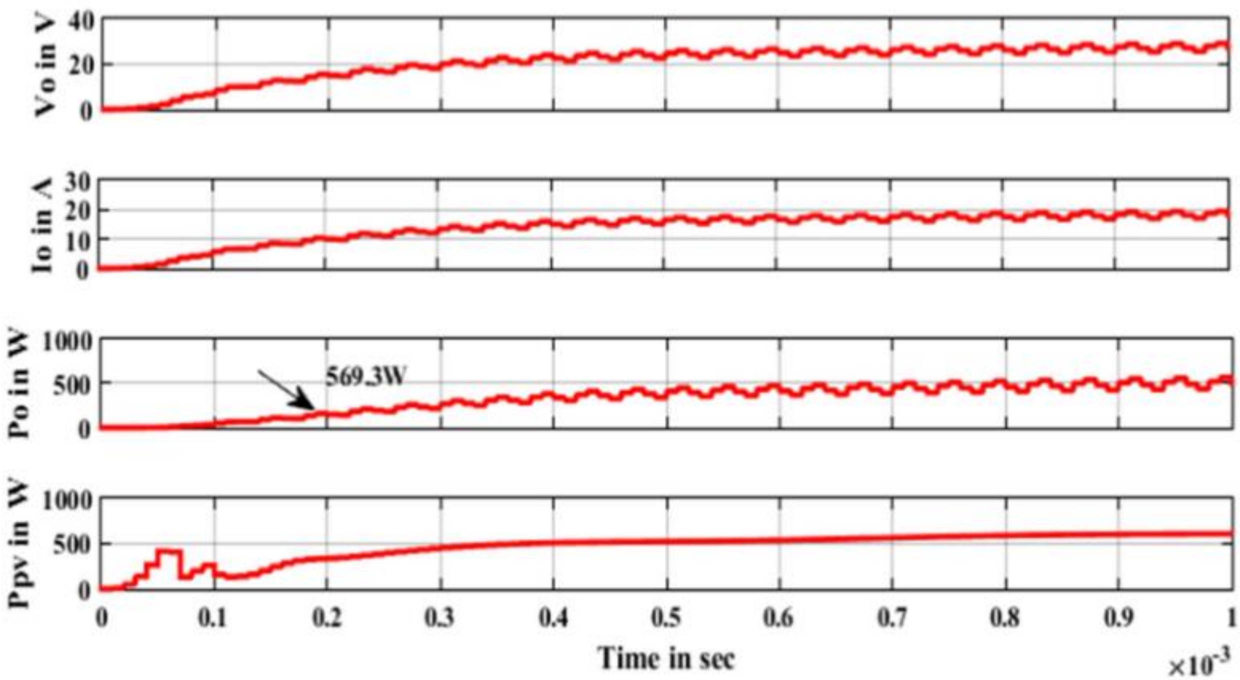

Figure 3.18: Output voltage, current, power and panel power of string architecture using PSO

It is noticed from the Figure 3.18 that power reaches it steady state value at time t=0.009s. The P-V features have a maximum power of 629.9 W. The power from the PV panels is 90.37 percent of full power by means of string architecture (629.9W).

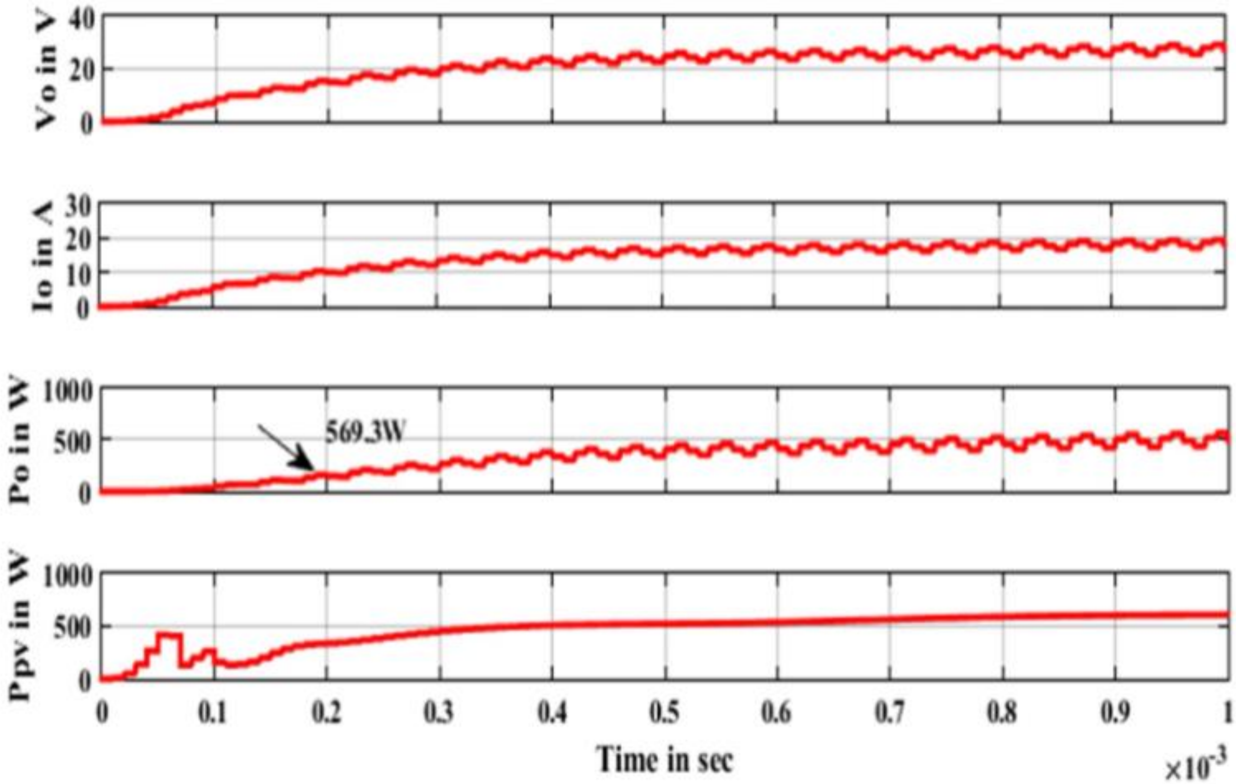

Figure 3.19: Output voltage, current, power and panel power of String architecture using RDPSO

From the simulation results, it is observed that 96.74% of power is extracted from the PV panels using the irradiance pattern 1 as shown in Figure 3.19. Both PSO and RDPSO algorithm extract the same amount of power from the PV panels but more oscillations in PSO compared to RDPSO.

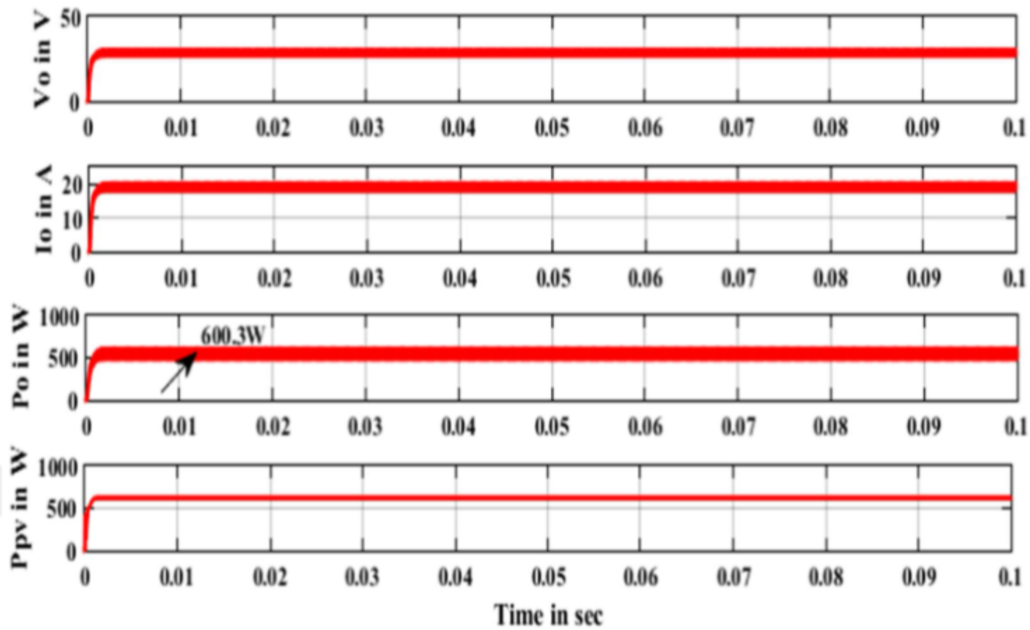

Figure 3.20: Output voltage, current and power of String architecture using GWO

It is observed from the simulation study that, the power obtained using GWO technique is 98.58% of its peak value (629.9W). When compared to PSO and RDPSO, GWO has fewer oscillations as presented in Figure 3.20 and the output power reaches its GPP very fast.

Figure 3.21: Performance of string architecture using PSO, RDPSO and GWO algorithms

P_{max} (W)	Algorithm	Architecture	V_{pv} (V)	I_{pv} (A)	P_{pv} (w)	V (V)	I_O (A)	P_o (w)	Converter Efficiency (%)	Tracking Efficiency (%)
629.9	PSO	String	31.81	20.16	609.4	28.26	18.84	569.3	93.43	96.74
	RDPSO		31.81	20.16	609.4	28.26	18.84	569.3	93.43	96.74
	GWO		30.82	20.78	621.0	29.02	19.35	600.3	96.67	98.58

It is clearly observed from the Table 3.21 that 98.58% of power is extracted from the PV panels using string architecture and it is also noticed that power reaches its GPP very fast in GWO algorithm when compared to PSO and RDPSO technique.

3.5.3 Differential Power Processing Architecture

In string architecture, the power loss in the same string is important under partial shading conditions. Four PV arrays are connected in series and each PV array is connected in series with DPP boost architecture to overcome this drawback. This arrangement is connected to a common boost converter and simulated using MATLAB. Simulation result shows that, DPP architecture is suitable for mismatched condition of PV array. If there is no mismatch in PV array the architecture is operated as a normal central architecture.

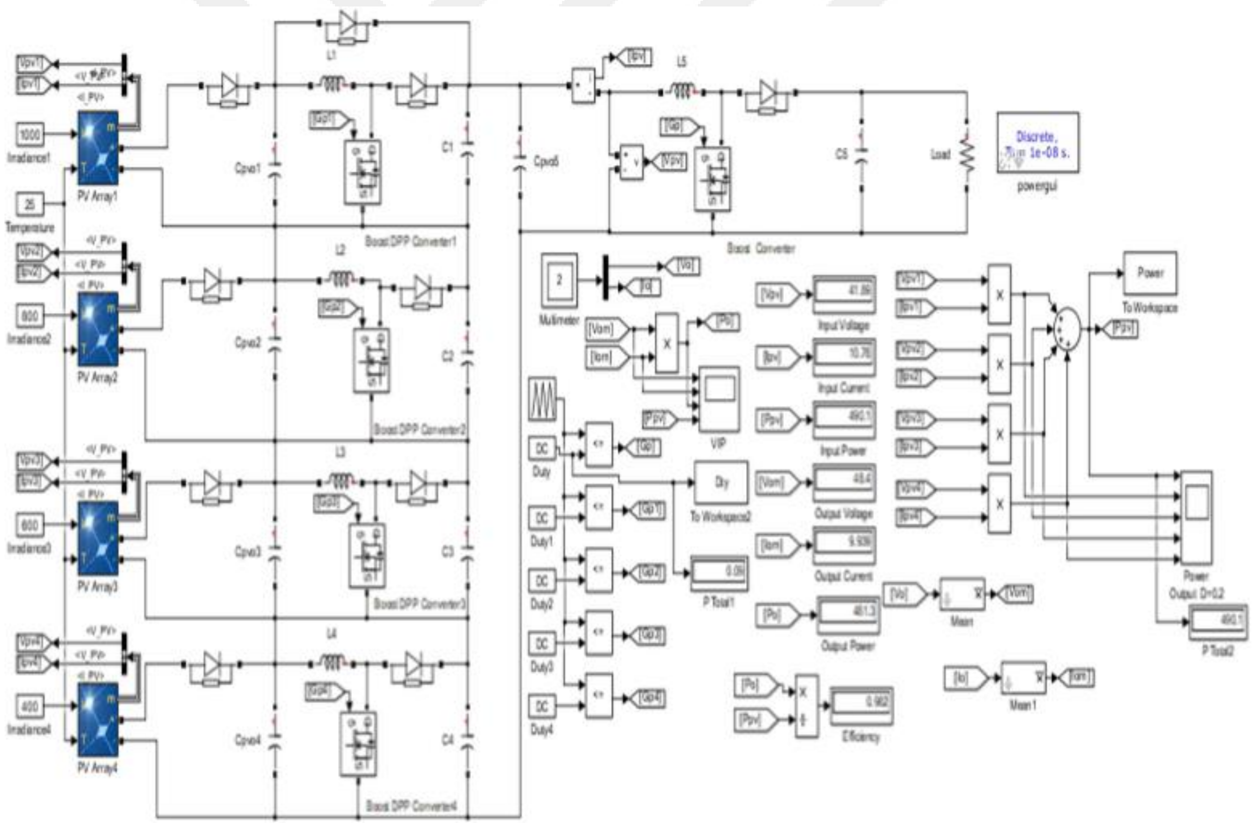

Figure 3.22: Simulink model for DPP architecture

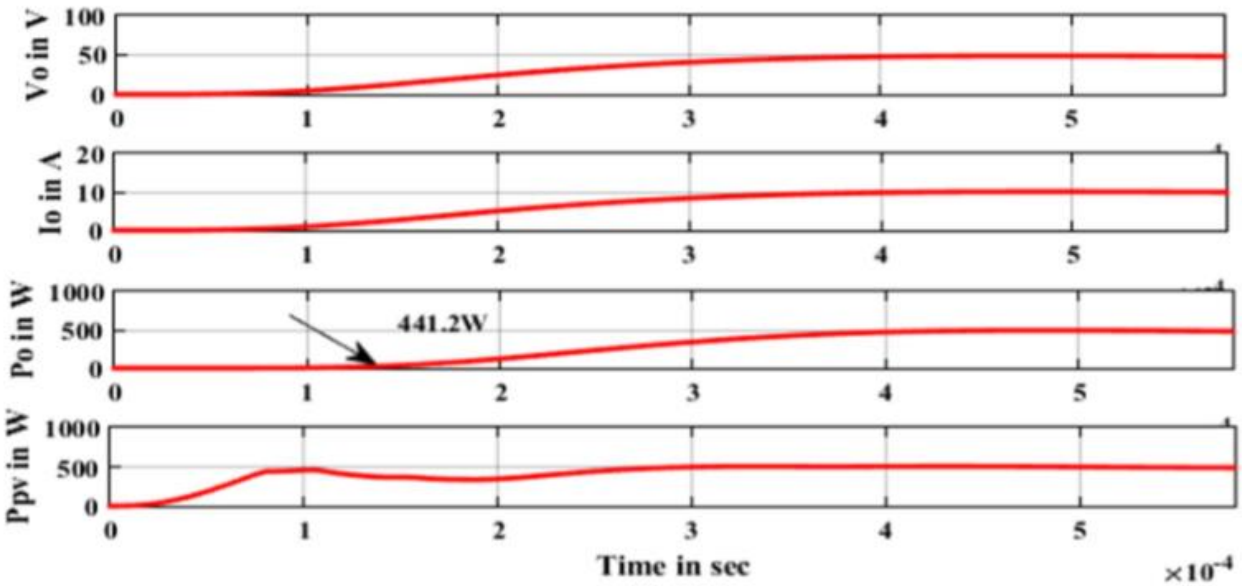

Figure 3.23: Output voltage, current, power and panel power of DPP architecture using PSO

Figure 3.23 presents the simulation result of PV array using PSO algorithm. From the results it is observed that the power from PV array reaches its GPP at t=0.009s. It is found that 99.81% of power is extracted from its maximum value.

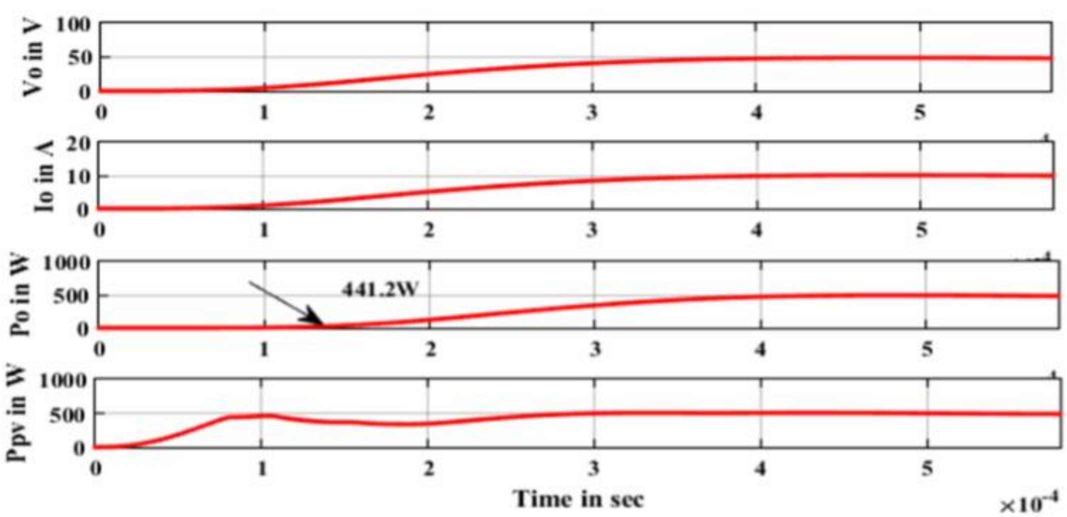

Figure 3.24: Output voltage, current, power and panel power of DPP architecture using RDPSO

In the simulation study, the output power obtained from the RDPSO algorithm reaches a steady state value at t= 0.031s as shown in Figure 4.24. It is found that 99.81% of power is extracted from its maximum power (491.2W).

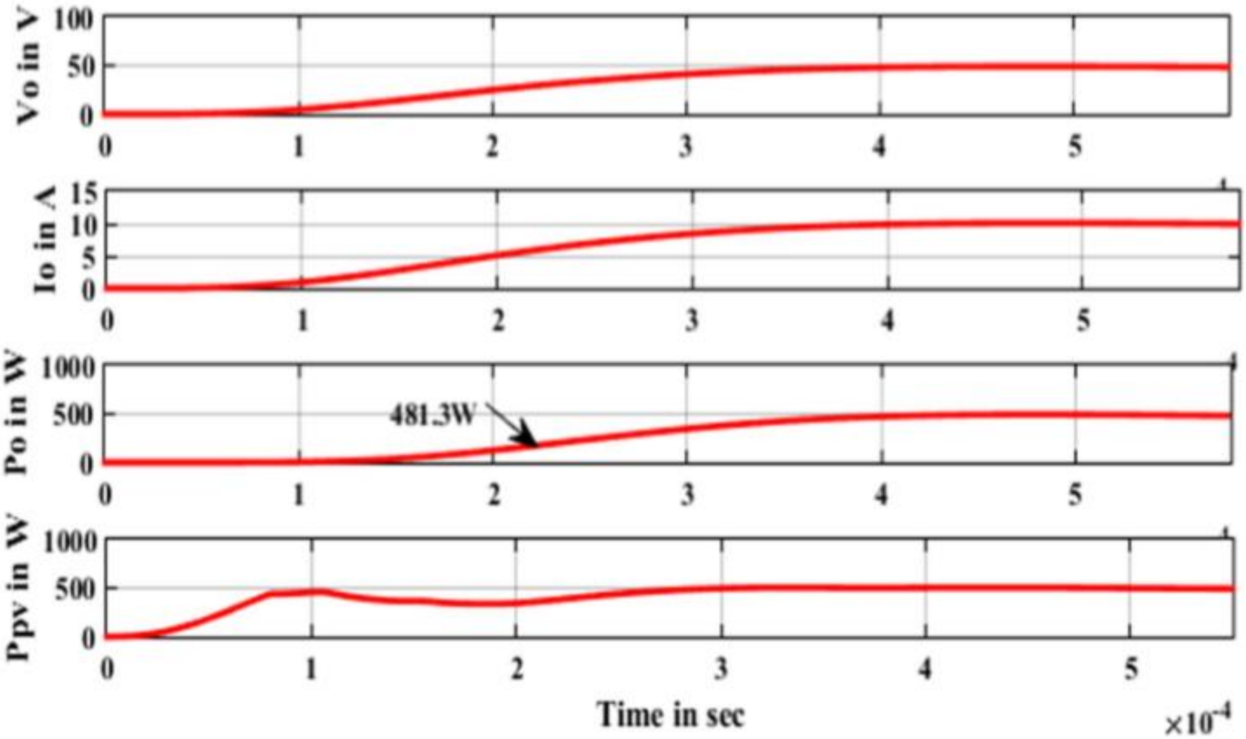

Figure 3.25: Output voltage, current, power and panel power of DPP architecture using GWO

The simulation result of Figure 3.25 shows the maximum power tracked from the P-V characteristic is 491.2W. DPP architecture using GWO extracts a maximum power from the PV array (99.91%) from its maximum value. The simulation results obtained from the PV panels using various algorithms are tabulated in Table 3.4. The power-voltage characteristics of DPP architecture is presented in Figure 3.26(a) and the convergence plot is presented in Figure 3.27(b).

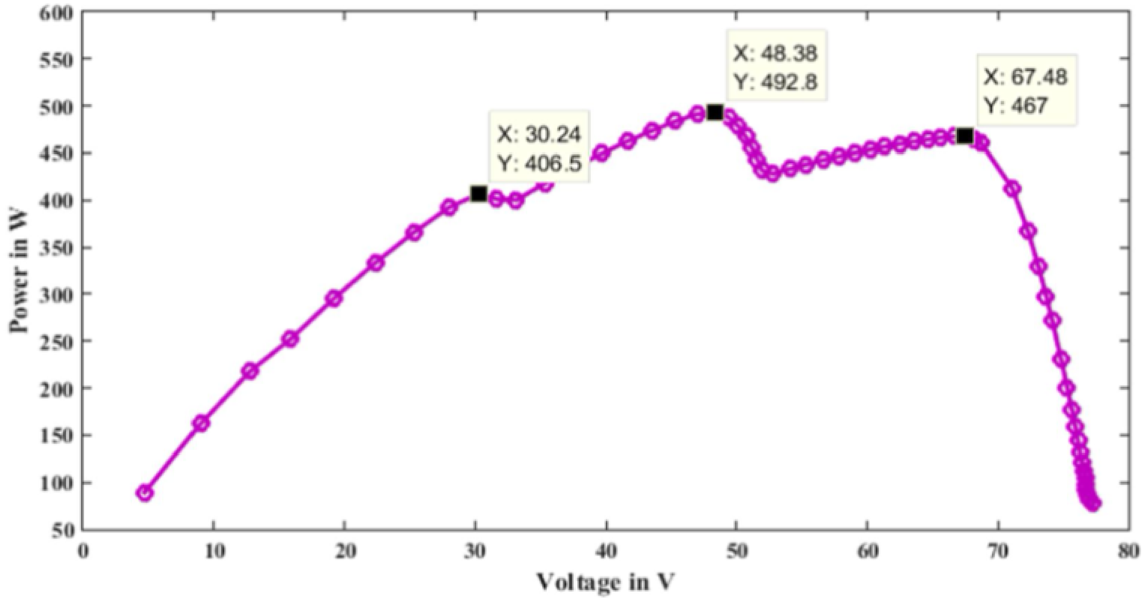

Figure 3.26:(a) Power-Voltage characteristics of DPP architecture

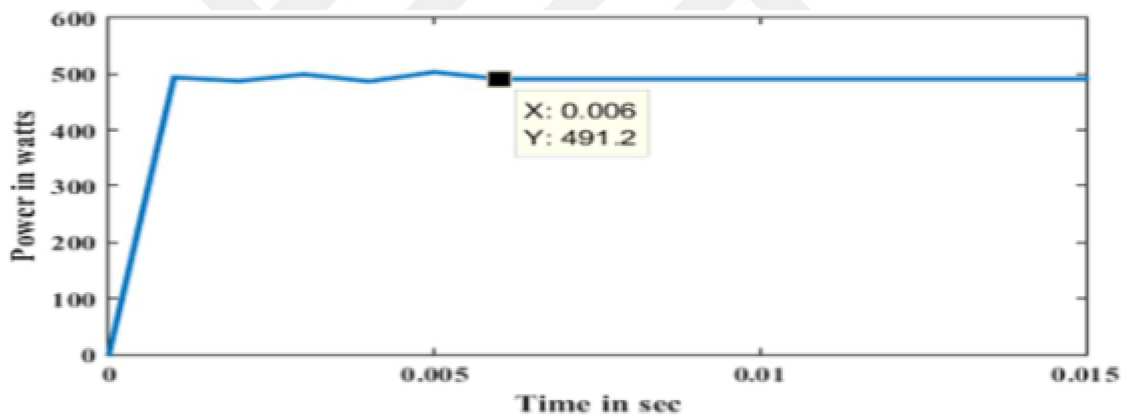

Figure 3.27: (b) Power Vs Time for DPP architecture

P_{max} (W)	Algorithm	Architecture	V_{pv} (V)	I_{pv} (A)	P_{pv} (w)	V (V)	I_O (A)	P_o (w)	Converter Efficiency (%)	Tracking Efficiency (%)
741.1	PSO	DPP	42.26	10.65	487.7	45.72	9.625	440.1	90.24	99.28
	RDPSO		42.21	10.66	487.4	45.70	9.621	439.7	90.20	99.22
	GWO		42.91	10.60	491.2	46.00	9.684	445.4	90.69	100

Table 3.3: Performance of DPP architecture using PSO, RDPSO and GWO algorithms

When compared to central and string, DPP architecture gives 445.4 W output power and 90.69% efficiency in GWO algorithm is compared to PSO, RDPSO.

In order to find the best results of central, string and DPP architectures, all the three architecture are combined and simulated using MATLAB/SIMULINK and the results are presented in Figures (3.29) to (3.30). The combined Simulink model using GWO technique is shown in Figure 4.23. All the architecture consists of four panels, its irradiance values are 1000W/m2, 800W/m2, 600W/m2 and 400W/m2 respectively. The temperature is 25C for all the panels and it is constant. The load is resistive, and its value is 10Ÿ. The duty value for boost converter is set as 0.1 for all the architecture in order to justify the results.

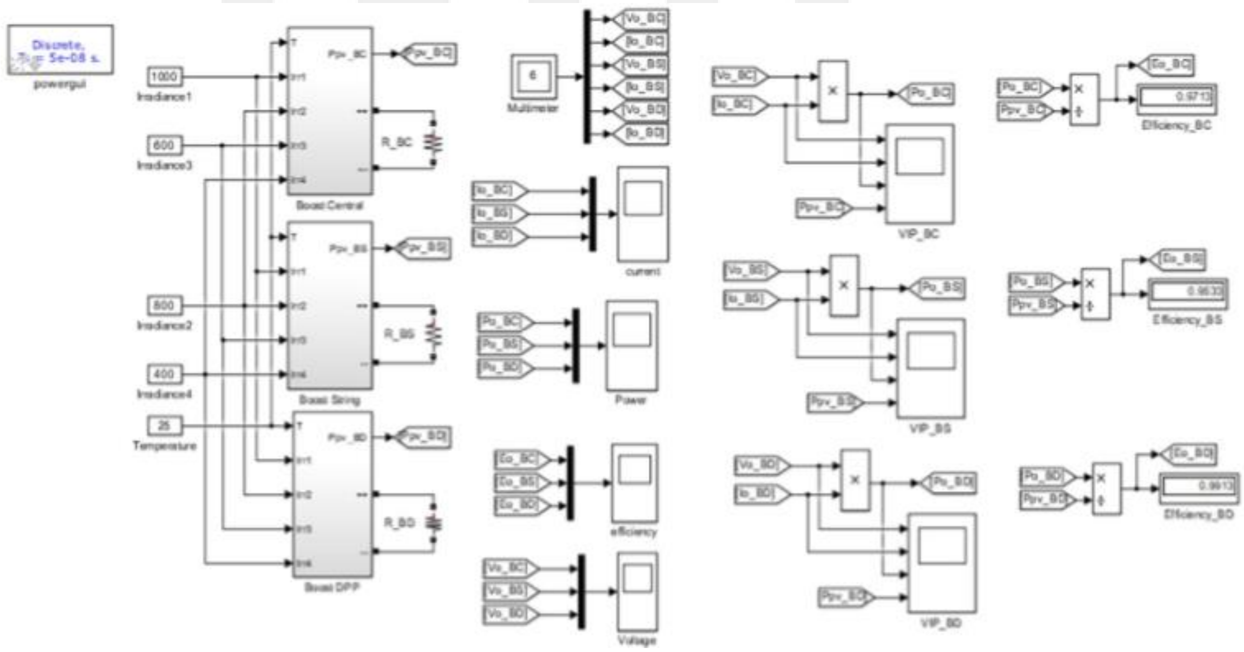

Figure 3.28: Combined Simulink model using GWO algorithm

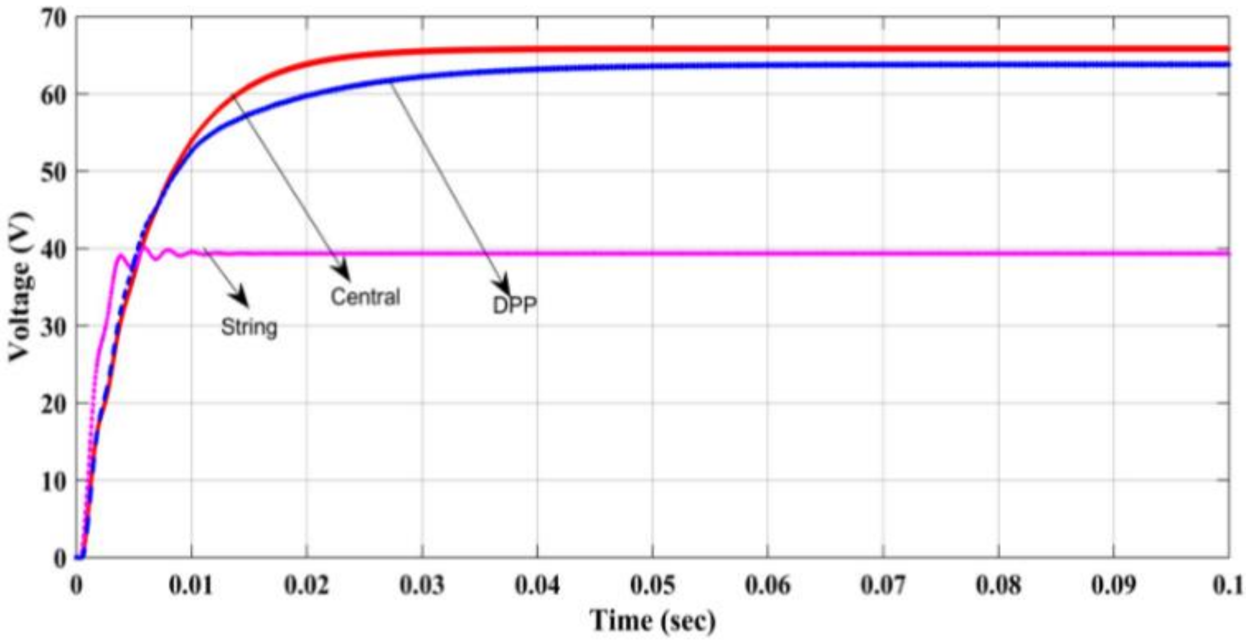

Figure 3.29: Output voltage for central, string and DPP architecture with GWO

Figure 3.29 Output voltage for central, string and DPP architecture with GWO. It is observed from the simulation study that central, string and DPP architecture has oscillations up to 0.008s,0.013s and 0.006 s respectively and it reaches its GPP at t=0.055s, 0.014s and 0.03s.

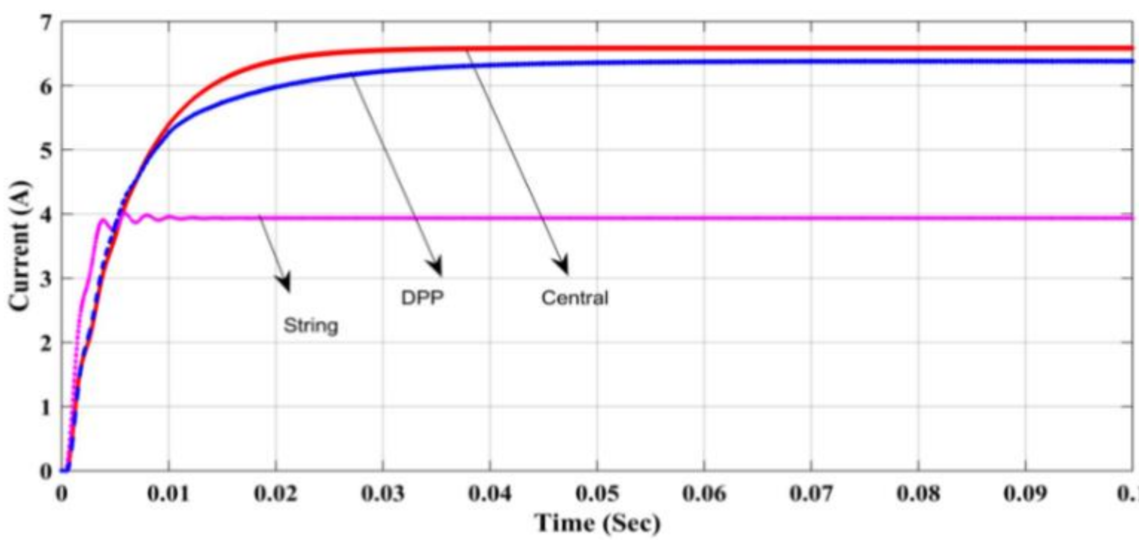

Figure 3.30: Output current for central, string and DPP architecture with GWO

The current value for central, string and DPP architecture is shown in Figure 3.30. From the results it is noticed that oscillations are present up to 0.009s, 0.012s, and 0.006s for central, string and DPP architecture. Almost 0.02s, 0.012s, 0.02s is taken by for central, string and DPP to reach the GPP.

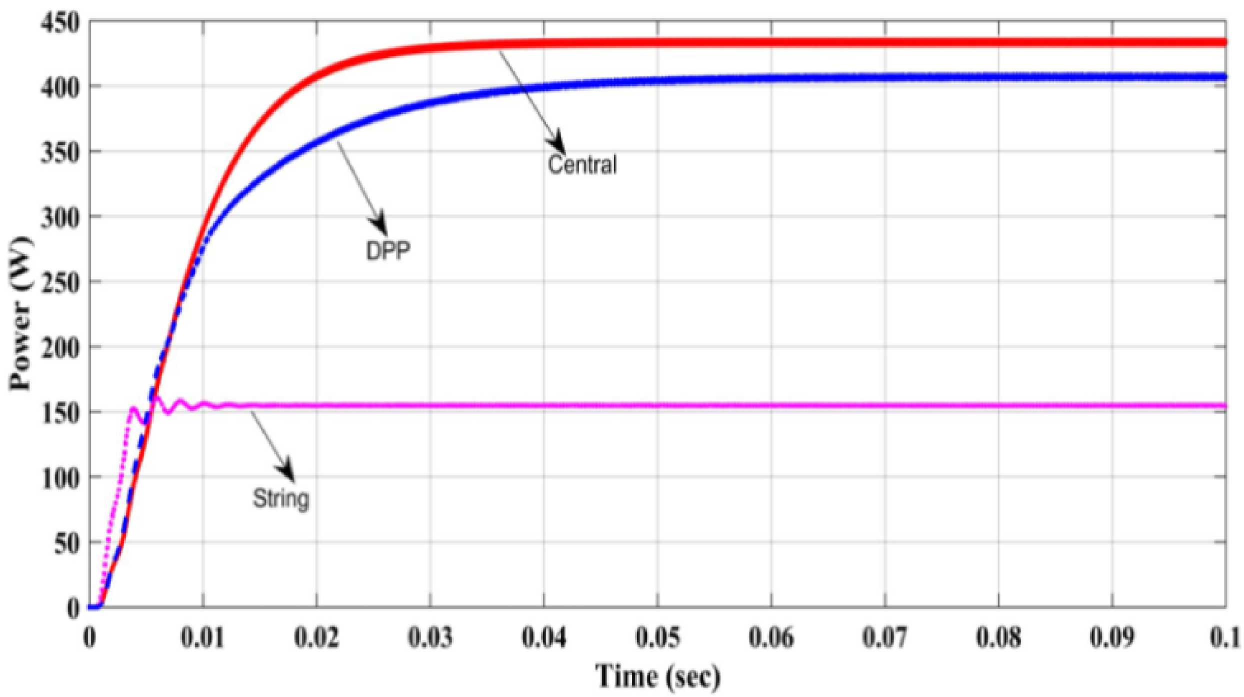

Figure 3.31: Output power for central, string and DPP architecture with GWO

The result shows that central, string and DPP architecture reaches its global power point at t=0.05s, 0.025s and 0.025s respectively. Also, oscillations are observed for central, string and DPP architecture are 0.009s, 0.011s and 0.006s respectively.

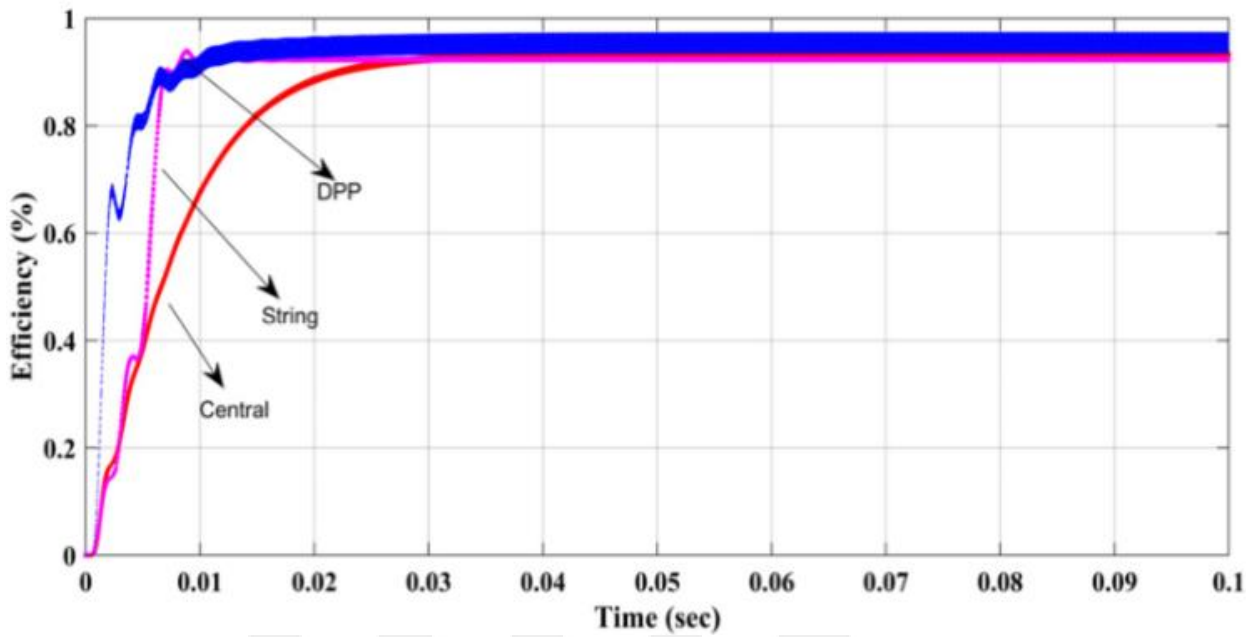

Figure 3.32: Efficiency for central, string and DPP architecture with GWO

From the simulation result, it is observed that DPP with GWO has 96.81% of efficiency and it is higher compared to central and string architecture. The values of voltage, current, power and efficiency are tabulated in Table 3.4.

Table 3.4: Performance of PV system with GWO using different architecture

Parameters	Algorithm	Central	String	DPP
Output Voltage (V)	GWO	**70.34**	**40.01**	**66.62**
Output Current (A)		**6.395**	**3.637**	**6.058**
Output Power (W)		**457.8**	**146.8**	**408.2**
Conversion Efficiency (%)		**97.13**	**95.33**	**99.13**

The performance of the PV array under PSC using various optimization algorithms with different architecture are tabulated in Table 3.5.

Table 3.5: Performance of architecture using PSO, RDPSO and GWO algorithms

Algorithms & Architecture		V_{pv} (V)	I_{pv} (A)	P_{pv} (w)	V (V)	I_O (A)	P_o (w)	Converter Efficiency (%)	Tracking Efficiency (%)
PSO	**Central**	**66.23**	**7.101**	**470.3**	**70.97**	**6.451**	**462.0**	**98.24**	**99.80**
	String	**31.81**	**20.16**	**609.4**	**28.26**	**18.84**	**569.3**	**93.43**	**96.74**
	DPP	**42.77**	**10.59**	**490.3**	**46.36**	**9.519**	**441.2**	**89.98**	**99.81**
RDPSO	**Central**	**66.23**	**7.101**	**470.3**	**70.97**	**6.451**	**462.0**	**98.24**	**99.80**
	String	**31.81**	**20.16**	**609.4**	**28.26**	**18.84**	**569.3**	**93.43**	**96.74**
	DPP	**42.77**	**10.59**	**490.3**	**46.36**	**9.519**	**441.2**	**89.98**	**99.81**
GWO	**Central**	**67.19**	**7.014**	**471.2**	**70.92**	**6.447**	**461.4**	**97.91**	**95.92**
	String	**30.32**	**20.78**	**621.0**	**29.02**	**19.35**	**600.3**	**96.67**	**98.58**
	DPP	**41.89**	**10.76**	**490.8**	**48.4**	**9.939**	**481.3**	**98.20**	**99.91**

3.6 CONCLUSION

Analysis of PV array under partial shading condition by employing different PV power processing architecture such as central, string and Differential Power Processing (DPP) architecture for boost converter with MPP optimization by Grey Wolf Optimization (GWO) algorithm and the results are compared with PSO and RDPSO. It has been noted that the GWO algorithm DPP architecture provides greater performance.

4. CONCLUSIONS AND FUTURE WORKS

4.1 CONCLUSION

This research work aims at enhancement of PV system under PSC by maintaining maximum power extraction irrespective of the changes in irradiance. In order to achieve this MPP and GPP tracking by various optimization techniques has been studied. The efficiency of PV system has also been analyzed by employing various architectures for boost converter.

Under Partial Shading Condition (PSC), the PV array exhibits local and Global Power Peak (GPP). Therefore, under PSC the GPP is tracked to achieve MPP. Tracking GPP is the main challenge under partial shading condition. To solve these problems, optimization strategies are used to control the GPP. Different strategies for optimizing particle swarm optimization (PSO), algorithm for gravitational search (GSA), etc., Random Drift PSO (RDPSO), Flower Pollination Algorithm (FPA) and Grey Wolf Optimization (GWO) have been tested to determine the best duty value for the boost converter to extract maximum power and the results are analyzed to select the best optimization algorithm for MPPT of PV system during PSC.

It is observed from the analysis that, the DPP architecture with GWO algorithm results in higher efficiency and output power and faster convergence. DPP architecture with GWO algorithm provides the maximum conversion efficiency of 98.2% and tracking efficiency of 99.91% which is higher when compared to all other algorithms hence DPP architecture with GWO algorithm is best suited for PSC.

4.2 SCOPE FOR FUTURE WORK

There is a wide scope for extending this research work by integrating the system with standalone load, grid, hybrid system etc. Some of the extensions of the research work are listed here.

1.In general, the commercial and domestic loads require AC supply, but the PV system generates DC supply and so the DC output of PV system can be inverted to AC using inverter and MPPT analysis for the PV inverter system can be performed.

2. In recent days, micro grids are developed by integrating two or more renewable energy sources forming a hybrid system as alternative to EB grid for villages. In such hybrid systems PSC PV system can be added as one of the sources and can be analyzed for MPPT.

3.The PV system cannot deliver energy to load throughout the day and so battery backup is necessary for PV based standalone system. In such systems a power management concept can be implemented so that maximum power is always fetched from PV and remaining from battery.

4.Recent trend is to feed energy from PV to grid when PV energy is not utilized by the consumer. In such systems PSC analysis can be performed for MPPT.

5. REFERENCES

[1] R. Karki and R. Billinton, “Reliability/cost implications of pv and wind energy utilization in small isolated power systems, ”IEEE Transactions on Energy Conversion, vol. 16, no. 4, pp. 368–373, 2001.

[2] H. Ravaee, S. Farahat, and F. Sarhaddi, “Artificial neural network based model of photovoltaic thermal (pv/t) collector, ”The Journal of Mathematics and Com-puter Science, vol. 4, no. 3, pp. 411–417, 2012.

[3] G. K. Singh, “Solar power generation by pv (photovoltaic) technology: a review, “Energy, vol. 53, pp. 1–13, 2013.

[4] S. R. Chowdhury and H. Saha, “Maximum power point tracking of partially shaded solar photovoltaic arrays,” Solar Energy Materials and Solar Cells,vol. 94, no. 9, pp. 1441–1447, 2010.

[5] R. Ramaprabha, M. Balaji, and B. Mathur, “Maximum power point tracking of partially shaded solar pv system using modified fibonacci search method with fuzzy controller,” International Journal of Electrical Power & Energy Systems, vol. 43, no. 1, pp. 754–765, 2012

[6] Kok Soon Tey & Saad Mekhilef, 2014, ‘Modified Incremental Conductance Algorithm for Photovoltaic System under Partial Shading Conditions and Load Variation’, IEEE Trans. on Industrial Electronics, vol. 61, no.10,pp.5384-5392.

[7] Dezso Sera, Laszlo Mathe, Tamas Kerekes, Sergiu Viorel Spataru & Remus Teodorescu, 2013, ‘On the Perturb and Observe and Incremental Conductance MPPT Methods for PV Systems’, IEEE Journal of Photovoltaic, vol. 3, no. 3,pp.1070 – 1078.

[8] Abdelaziz Youcef, Abdallah Miloudi, Rafik Sayah & Houari Sayah, 2016 ‘Optimization of partially shaded PV array using a modified P&O MPPT algorithm’, Leonardo Electronic Journal of Practices and Technologies, no. 28, pp.179-196.

[9] Alajmi, BN, Ahmed, KH, Finney, SJ & Williams, BW 2013. ‘A Maximum Power Point Tracking Technique for Partially Shaded Photovoltaic Systems in Microgrids’, IEEE Transactions on Industrial Electronics, vol. 60, no. 4, pp. 1596-1606.

[10] Alireza Ramyar, Hossein Iman-Eini & Shahrokh Farhangi 2017, ‘Global Maximum Power Point Tracking Method for Photovoltaic Arrays Under Partial Shading Conditions’, IEEE Transactions on Industrial Electronics, vol. 64, no. 4,pp.2855 – 2864.

[11] Zainal Salam, Zulkifli Ramli, Jubaer Ahmed & Muhammad Amjad 2015, ‘Partial Shading in Building Integrated PV System: Causes, Effects and Mitigating Techniques’, International Journal of Power Electronics and Drive System, vol. 6, no. 4, pp. 712-722.

[12] Esmat Rashedi, Hossein Nezama badi-pour &Saeid Saryadi 2009, 'A Gravitational Search Algorithm', Information Sciences, vol. 179, pp. 2232-2248.

[13] Tat Luat Nguyen & Kay-Soon Low 2010, 'A global maximum power point tracking scheme employing direct search algorithm for photovoltaic systems', IEEE Trans. Ind. Electron., vol. 57, no. 10, pp.3456-3467.

[14] Ishaque, K, Salam, Z, Amjad, M & Mekhilef, S 2012, 'An improved particle swarm optimization (PSO) based MPPT for PV with reduced steady-state oscillation', IEEE Trans. Power Electronics., vol. 27, no. 8, pp. 3627-3638.

[15] Ishaque, K, Salam, Z, Amjad, M & Mekhilef, S 2012, 'An improved particle swarm optimization (PSO) based MPPT for PV with reduced steady-state oscillation', IEEE Trans. Power Electronics., vol. 27, no. 8, pp. 3627-3638.

[16] Taisir Eldos & Rose Al Qasim 2013, 'On the performance of the gravitational search algorithm', Internal Journal of Advanced Computer Science and Applications, vol. 4, no. 8, pp.74-78

[17] Yiqiong Yuan, Jun Sun, Dongmei Zhou & Jianan Sun, 2016, 'Multi-Objective Random Drift Particle Swarm Optimization Algorithm Based on RDPSO and Crowding Distance Sorting', World Academy of Science, Engineering and Technology International Journal of Mathematical, Physical, Electrical and Computer Engineering, vol. 10, no. 4, pp 183.

[18] Satyajit Mohanty, Bidyadhar Subudhi & Pravat Kumar Ray 2016 'A New MPPT Design Using Grey Wolf Optimization Technique for Photovoltaic System under Partial Shading Conditions', IEEE Trans. on Sustainable Energy, vol. 7, no. 1, pp.181-188.

[19] Ramdan B. A. Koad & Ahmed F Zobaa, 2014, 'Comparison between the Conventional Methods and PSO Based MPPT Algorithm for Photovoltaic Systems', International Journal of Electrical, Robotics, Electronics and Communications Engineering, vol. 8, no. 4, pp.690-695.

[20] Ahmed A, Elserougi, Mohamed S, Diab, Ahmed M, Massoud, Ayman S, Abdel-Khalik & Shehab Ahmed 2015, 'A Switched PV Approach for Extracted Maximum Power Enhancement of PV Arrays During Partial Shading', IEEE Transactions on Sustainable Energy, vol. 6, no. 3, pp.767 – 772.

[21] Prasanth Ram, J & Rajasekar, N 2017, 'A Novel Flower Pollination Based Global Maximum Power Point Method for Solar Maximum Power Point Tracking', IEEE Transactions on Power Electronics, vol. 32, no. 11, pp.8486-8499.

[22] Pradeep S Shenoy & Philip T Krein 2013, 'A Differential Power Processing for DC Systems', IEEE Trans. Power Electron., vol. 28, no. 4, pp. 1795-1806.

[23] JaberA Abu Qahouq & Yuncong Jiang 2014, ‘Distributed photovoltaic Solar System Architecture with Single Power Converter and Single Sensor Single Maximum Power Point Tracking Controller’, IET Power Electronics, vol. 7, no. 10, pp. 2600-2609.

[24] Binjie Gu & Feng Pan 2013, ‘Modified Gravitational Search Algorithm with particle memory ability and its application’, International Journal of Innovative Computing, Information and Control, vol. 9, no. 11, pp. 4531-4544.

[25] Kyoung-Tak Kim & Joung-Hu Park 2017, ‘Multi-output differential power processing system using boost-flyback converter for voltage balancing’, International conference on recent advances in Signal Processing, Telecommunications and Computing, pp. 139-142.

[26] Seyedali Mirjalili 2014, ‘Grey Wolf Optimizer’, Advances in Engineering Software, vol. 69, pp. 46-61.

[27] Yi-Hwa, Shyh-Ching Huang Jia-Wei Huang & Wen-Cheng Liang, 2012, ‘A Particle Swarm Optimization based Maximum Power Point Tracking Algorithm for PV Systems Operating under Partially Shaded Conditions’, IEEE Trans. on Energy Conversion, vol. 27, no. 4, pp.1027-1035.

[28] Rui Wang, Yongquan Zhou, Shilei Qiao & Kang Huang 2016, ‘Flower pollination algorithm with Bee Pollinator for cluster analysis’, Elsevier vol. 116, no.1, pp. 1-14.

[29] W. Xiao, Photovoltaic Power System: Modeling, Design, and Control. John Wiley& Sons, 2017.

[30] N. Femia, G. Petrone, G. Spagnuolo, and M. Vitelli, Power electronics and control techniques for maximum energy harvesting in photovoltaic systems. CRC press,2012.

[31] M. Villalva, J. Gazoli, and E. Filho, “Comprehensive approach to modeling and simulation of photovoltaic arrays,”IEEE Trans. Power Electron., vol. 24, no. 5, pp.1198–1208, May 2009.

[32] S. Shongwe and M. Hanif, “Comparative analysis of different single-diode pv modeling methods,”IEEE J. Photovoltaics, vol. 5, no. 3, pp. 938–946, May 2015.

[33] M. C. D. Piazza, M. Luna, G. Petrone, and G. Spagnuolo, “Translation of the single-diode pv model parameters identified by using explicit formulas, IEEE J. Photovoltaics, vol. 7, no. 4, pp. 1009–1016, Jul. 2017.

[34] R. Teodorescu, M. Liserre, and P. Rodriguez, Grid converters for photovoltaic and wind power systems. John Wiley & Sons, 2011, vol. 29.

[35] N. Karami, N. Moubayed, and R. Outbib, “General review and classification of different mppt techniques, “Renew. Sust. Energy Rev., vol. 68, pp. 1–18, 2017.

[36] L. V. Hartmann, M. A. Vitorino, M. B. d. R. Correa, and A. M. N. Lima, “Com-bining model-based and heuristic techniques for fast tracking the maximum-power point of

photovoltaic systems,”IEEE Trans. Power Electron., vol. 28, no. 6, pp.2875–2885, Jun. 2013.

[37] Y. Mahmoud, M. Abdel wahed, and E. F. El-Saadany, “An enhanced mppt method combining model-based and heuristic techniques,”IEEE Trans. Sustain. Energy, vol. 7, no. 2, pp. 576–585, Apr. 2016.

[38] L. Cristaldi, M. Faifer, M. Rossi, and S. Toscani, “An improved model-based maximum power point tracker for photovoltaic panels,” IEEE Trans. Instrum. Meas .,vol. 63, no. 1, pp. 63–71, Jan. 2014.

[39] E. Bianconi, J. Calvente, R. Giral, E. Mamarelis, G. Petrone, C. A. Ramos-Paja,G. Spagnuolo, and M. Vitelli, “A fast current-based mppt technique employing sliding mode control, IEEE Trans. Ind. Electron., vol. 60, no. 3, pp. 1168–1178, Mar. 2013.

[40] Y. Hu, W. Cao, J. Wu, B. Ji, and D. Holliday, “Thermography-based virtual mppt scheme for improving pv energy efficiency under partial shading conditions,” IEEE Trans. Power Electron., vol. 29, no. 11, pp. 5667–5672, Nov. 2014.

[42] N. Femia, G. Petrone, G. Spagnuolo, and M. Vitelli, “Optimization of perturb and observe maximum power point tracking method,” IEEE Trans. Power Electron., vol. 20, no. 4, pp. 963–973, Jul. 2005.

[43] X. Li and H. Wen, “Evaluation of different maximum power point tracking techniques by using en 50530 dynamic test standard,” in2016 IEEE International Conference on Power Electronics, Drives and Energy Systems (PEDES), Dec. 2016, pp.1–6.

[44] M. Sokolov and D. Shmilovitz, “A modified mppt scheme for accelerated convergence,” IEEE Trans. Energy Convers., vol. 23, no. 4, pp. 1105–1107, Dec. 2008.

[45] V. V. R. Scarpa, S. Buso, and G. Spiazzi, “Low-complexity mppt technique exploit-ing the pv module mppt locus characterization,” IEEE Trans. Ind. Electron, vol. 56, no. 5, pp. 1531–1538, May. 2009.

[46] Y.-H. Liu and J.-W. Huang, “A fast and low-cost analog maximum power point tracking method for low power photovoltaic systems, “Sol. Energy, vol. 85, no. 11, pp. 2771–2780, 2011.

[47] S. Jain and V. Agarwal, “A new algorithm for rapid tracking of approximate maximum power point in photovoltaic systems,” IEEE Power Electron. Lett., vol. 2, no. 1, pp. 16–19, Mar. 2004.

[48] Ahmed A, Elserougi, Mohamed S, Diab, Ahmed M, Massoud, Ayman S, Abdel-Khalik & Shehab Ahmed 2015, ‘A Switched PV Approach for Extracted Maximum Power Enhancement of PV Arrays During Partial Shading’, IEEE Transactions on Sustainable Energy, vol. 6, no. 3,pp.767 – 772

[49] Hyunji Lee & Katherine A Kim 2016, 'Differential Power Processing Converter Design for Photovoltaic Wearable Applications', IEEE 8th International Power Electronics and Motion Control Conference (IPEMC-ECCE Asia).

[50] Pradeep S Shenoy & Philip T Krein 2013, 'A Differential Power Processing for DC Systems', IEEE Trans. Power Electron., vol. 28, no. 4, pp. 1795-1806.

[51] Ahmed A, Elserougi, Mohamed S, Diab, Ahmed M, Massoud, Ayman S, Abdel-Khalik & Shehab Ahmed 2015, 'A Switched PV Approach for Extracted Maximum Power Enhancement of PV Arrays During Partial Shading', IEEE Transactions on Sustainable Energy, vol. 6, no. 3, pp.767 – 772.

[52] Kyoung-Tak Kim & Joung-Hu Park 2017, 'Multi-output differential power processing system using boost-flyback converter for voltage balancing', International conference on recent advances in Signal Processing, Telecommunications and Computing, pp. 139-142.